공학석사 학위논문

Study on ventilation rate estimation of mechanically ventilated broiler house

강제환기식 육계사의 환기량 산정 방안 연구

2018년 2월

서울대학교 대학원
생태조경 · 지역시스템공학부
지역시스템공학전공

박 관 용

Study on ventilation rate estimation of mechanically ventilated broiler house

강제환기식 육계사의 환기량 산정 방안 연구

지도교수 이 인 복

이 논문을 공학석사 학위논문으로 제출함

2018 년 2 월

서울대학교 대학원
생태조경 · 지역시스템공학부 지역시스템공학전공
박 관 용

박관용의 공학석사 학위논문을 인준함
2018 년 2 월

위 원 장 _____(인)

부위원장 _____(인)

위 원 _____(인)

Abstract

The percentage share of the livestock industry output value of Korean agriculture has been steadily increasing since the 1990s. Among them, the chicken production has been increasing as consumption per capita. Broiler houses had been increased their scale and breeding density in order to meet the chicken consumption. However, dense breeding density causes accumulation of heat, moisture, and contaminants inside the broiler house. The improper environment in broiler house leads to a decline in productivity. Various problems can occur because of the failure of environmental control, such as dehydration due to the high temperature and low humidity, and proliferation of pathogenic microorganisms due to excessive humidity, and weakening of broiler's immunity due to the accumulation of pollutants.

Mechanically ventilation system and automatic control system were being introduced into broiler houses, to improve production efficiency through precise environmental control. Mechanically ventilated broiler house has an advantage in terms of controlling ventilation, which is the main environmental control mechanism in livestock houses. Heat, moisture, and pollutants generated inside the broiler house are discharged through ventilation. In order to discharge appropriate amount of substance, accurate evaluation of the ventilation rate is required. The ventilation control in mechanically ventilated broiler house is based on maximum airflow of exhaust fans currently. However, the actual airflow of the fan is reduced as the inlet area of facility decreases and thus static pressure difference between inside and outside of the facility increases. In consideration of this phenomena, evaluating method of ventilation rate was proposed using a fan performance curve, which is the ventilation characteristic of the exhaust fan and orifice equation, ventilation characteristic of the inlet. The in-situ fan performance curve and the discharge coefficient, which is the coefficient of orifice equation have to be evaluated in order to estimate the exact amount of ventilation rate in the broiler house.

In this study, ventilation rate was evaluated according to the operating conditions of the ventilating facility, in two mechanically ventilated broiler houses. Reduction of ventilation rate to set value was measured in the Ire broiler farm located in Buyeo, Chungcheongnam-do. The airflow of sidewall fans was measured according to the operating fans, under slot opening condition of winter. As a result, average airflow through target sidewall fan decreased as the number of operating fans increase. Measured ventilation rate when all three sidewall fans

were operated was 77.0% of the set ventilation rate. The slot opening, inlet of target broiler house was 25% open during the experiment. It was analyzed that the static pressure difference due to the narrow slot opening area reduced ventilation rate by acting as a load on the exhaust fans.

Experiment for evaluating ventilation characteristic was conducted in mechanically ventilated broiler house located in Gimje, Jeollabuk-do. The ventilation rate of tunnel fan and the static pressure difference between inside and outside of target broiler house were measured according to the ventilation operating condition, a number of operating fans and slot opening area. Computational fluid dynamics model of target broiler house was designed to overcome the limitation of the field experiment. As a result of regression analysis of the airflow for model validation, a significant difference between measured and simulated airflow was not observed (p-value = 0.239).

The measured ventilation rate and static pressure difference were analyzed to calculate the ventilation characteristic of target broiler house: in-situ fan performance curve and the discharge coefficient. The static pressure difference of in-situ fan performance curve was average 33.7 Pa low than design fan performance curve provided by the manufacturer. Computational fluid dynamics results showed low static pressure difference of in-situ fan performance curve was due to the distribution of static pressure. The static pressure difference between inlet and outlet of exhaust fans was relatively high according to the design fan performance curve. On the other hand, in most of the remaining space including the measurement position of the experiment, constant and low static pressure difference was formed. Computational fluid dynamics models of broiler houses with different lengths were additionally designed. A significant difference between simulated fan performance curve by broiler house length was not calculated (p-value = 0.189). Therefore, the in-situ fan performance curve was analyzed to be a unique characteristic of the target exhaust fan. The discharge coefficients were calculated 0.344 to 0.743 according to the slot opening area. The measured discharge coefficients were 5.29%–114.3% of widely used discharge coefficient of the vent (0.65). For the general application of the discharge coefficient, regression analysis was conducted. The linear relationship between the discharge coefficient and slot opening area was derived (R^2 = 0.851). Ventilation rate formula was derived from in-situ fan performance curve and orifice equation. It is expected that the ventilation rate can be calculated by a number of operating fans and slot opening area through the estimation formula proposed in this study, instead of field measurement using expensive equipment.

Keyword: Computational fluid dynamics, Discharge coefficient, Fan performance

curve, Mechanical ventilation, Broiler house, Orifice equation

Student Number: 2016-21704

Contents

List of figures

List of tables

Chapter 1. Introduction

The Korean livestock industry had been growing steadily due to the westernization of diet and increase in meat consumption, with production amounted 19.2 trillion won in 2016 (Ministry of Agriculture, Food and Rural Affairs, 2017). In particular, the consumption of chicken has been steadily increasing, and it is expected to rise from 13.9 kg per capita in 2016 to 14.6 kg per capita in 2026 (Korean Rural Economic Institute, 2017). Livestock houses, including broiler houses, have increased productivity by enlargement and concentrated animal feeding operation (CAFO), in response to the increasing demand (Kwon et al., 2014). The number of large-scale broiler farms breeding over 30,000 heads increased from 1,100 farms in 2000 to 2,116 farms in the second quarter of 2017 (Statistics Korea, 2017).

However, the introduction of CAFO placed a burden on control of the internal environment, causing accumulation of heat, moisture, dust, and hazardous gas inside the livestock houses. The result of an experiment of Bombik et al. (2011) showed that broiler houses exceeding optimum breeding density (18.6 heads m□²) had large deviation of air temperature and humidity and 1.6% higher mortality rate than control group (16.5 heads m□²). Air temperature and humidity in livestock houses are factors that have a large effect on productivity. In particular, chickens are sensitive to thermal stress, and their physiological and immune responses are strongly influenced by temperature (Lara & Rosagno, 2013). Humidity is also a major concern because too-low humidity causes dehydration of broilers and excessive humidity promotes the propagation of pathogenic microorganisms.

Ventilation is the key mechanism for environmental control of livestock facilities, including broiler houses. Ventilation is conducted to remove heat, moisture, and hazardous substances generated inside the facility through air exchange. If the required ventilation is not achieved, pollutants accumulation problem may occur. If excessive ventilation is carried out in the winter season, internal temperature and humidity less than the appropriate environment can occur. In order to precisely control the internal environment, mechanically ventilated broiler houses have been introduced, which have advantages over the conventional natural ventilation system (Kwon et al., 2014). Ventilation rate of a mechanically ventilated broiler house is controlled based on the maximum airflow of the exhaust fans at present. On the other hand, slot openings are controlled to maintain the static pressure difference inside and outside of the broiler house, independently of the ventilation rate. However, the actual ventilation rate of a mechanically ventilated broiler house varies depending on the static pressure difference. The relationship between airflow and static pressure difference is quantitatively

expressed by fan performance curve at exhaust fan and orifice equation at slot opening. Therefore, the ventilation rate of the mechanically ventilated broiler house can be calculated by combining two equations. It is reported that the fan performance is degraded when installed in the field, compared to the design fan performance curve. The discharge coefficient, which is the coefficient of the orifice equation, changes according to the area and shape of the opening. Therefore, in-situ fan performance curve and discharge coefficient have to be evaluated by field experiment in order to estimate the ventilation rate accurately.

A number of previous studies have been conducted to evaluate the ventilation rate of mechanically ventilated broiler houses. Devices such as averaging Pitot tube and airflow station (Lakenman et al., 2004; Segura et al., 2005), hot wire anemometer (Calvet et al., 2010), and the Fan Assessment Numeration System (FANS; Gates et al., 2004; Liang et al., 2013) have been used for measuring airflow of the exhaust fan. However, direct measurement methods using these devices are not suitable for long-term monitoring in terms of the cost and time. Measurement devices such as FANS require high cost and complicated measurement procedures and may hinder the ventilation of the target facility. Therefore, it is considered that the calculating ventilation rate by in-situ fan performance curve and orifice equation is most suitable for the operation of broiler house.

Meanwhile, studies on the livestock facilities have been actively conducted through computational fluid dynamics (CFD) for analyzing internal aerodynamic environment and ventilation characteristics. A field experiment for setting boundary conditions and model validation should be preceded for the CFD analysis, but it is possible to simulate environment of target facility considering the complex factors such as operating conditions and external weather. However, previous research on CFD modeling of livestock facilities set airflow of exhaust fan as maximum performance (Mostafa et al., 2012; Kwon et al., 2015) or measured values for single operating conditions, which means changes of ventilation rate according to the static pressure have not been considered. In order to improve the accuracy of the CFD model for mechanically ventilated livestock house, it is required to evaluate the ventilation rate according to the operating condition of the facility by applying the fan performance curve and orifice equation.

In this study, ventilation characteristics of a target mechanically ventilated broiler house were evaluated. In order to quantify ventilation characteristics, the airflow of the exhaust fan and the static pressure difference between inside and outside of the broiler house was measured. The in-situ fan performance curve of target tunnel fans and discharge coefficient of slot opening were evaluated by analyzing experimental results. The applicability of fan performance curve and

orifice equation in the CFD model was evaluated, and ventilation rate and static pressure distribution were analyzed by CFD simulation. Finally, the ventilation rate formula according to the number of operating fans and slot opening area was derived from in-situ fan performance curve and orifice equation.

Chapter 2. Literature Review

2.1. Evaluating method for ventilation rate of livestock houses

The ventilation rate of a broiler house can be evaluated by measuring mass flow rate (MFR) and measuring local ventilation rate inside the facility. The exhaust fan is the main mechanism of ventilation in the broiler house. Applying mechanical ventilation using an exhaust fan, the airflow can be controlled quantitatively and easily measured in comparison with a natural ventilation system. Calvet et al. (2010) measured a velocity of exhaust fan in mechanically ventilated broiler house by 16 measurements using a hot wire anemometer. The uncertainty of the airflow measurement was evaluated as less than 10% by numerical Monte Carlo method. An exhaust fan generates an airflow with non-uniform velocity distribution. Therefore, the point measurement using an anemometer has the possibility of error according to the measurement position; thus, repeated measurement is required for accurate measurement.

Various airflow measurement methods have been applied to complement the uncertainty and inconvenience of the multi-point measurement method. Among them, FANS suggested by Gates et al. (2004) is known as the most accurate method for measuring the airflow of the exhaust fan. FANS evaluates the distribution of air velocity by a propeller anemometer moving on a plane adjacent to the exhaust fan, and the static pressure difference between inside and outside of the facility is measured at the same time. FANS has high accuracy, with uncertainty less than 3% (Casey et al., 2007; Calvet et al., 2013), and applied in verification of other ventilation rate measurement methods, estimation of gas emission, and so on (Gates et al., 2005; Xin et al., 2009; Morello et al., 2014). However, FANS has not been commercialized at present because of its complicated structure. Averaging Pitot tube (APT) and airflow station are uncomplicated airflow measurement devices using Pitot tube. Lakenman et al. (2004) and Segura et al. (2005) studied the applicability of airflow measurement with APT in a swine house. Liang et al. (2013) measured airflow of the exhaust fan (diameter 0.91 m) installed in a broiler house using APT, and the error was about 4% compared with the airflow measured by FANS.

The method measuring the airflow of the exhaust fan can evaluate total ventilation rate of the mechanically ventilated livestock house relatively accurately but is not applicable to naturally ventilated facilities. Ventilation rate evaluating methods applicable to naturally ventilated livestock houses include heat, moisture, and CO_2 balance method, tracer gas method, and CFD. The balance method is a ventilation rate calculation method considering the conservation of mass or energy

of the target substance. Calvet et al. (2001) evaluated CO_2 generation from broiler and bedding material according to the activity of the broiler for the application of the CO_2 balance method to a broiler house. Winkel et al. (2015) estimated dust emission by measuring ventilation rate and dust concentration in a number of poultry, pig, and cattle houses. The ventilation rate of mechanically ventilated pig houses was evaluated by measuring airflow of exhaust fans. However, the ventilation rate of broiler and cattle house was evaluated by the CO_2 balance method, since the diameter of exhaust fans varied and some of them conducted natural ventilation. The balance method estimates ventilation rate based on generation rate and concentration of target substance; thus an error may occur if a precise evaluation of generation is not preceded. Pederson et al. (1998) conducted sensitivity analysis and evaluated by measuring the error of heat, moisture, and CO_2 balance method as 3.2–6.9% in the winter season and 11.6–23.9% in the summer season.

The tracer gas method is a method for evaluating ventilation rate by monitoring the concentration of low reactive gases such as carbon dioxide and sulfur hexafluoride. The local ventilation rate, as well as total ventilation rate of a target facility, can be measured by the tracer gas method. Since the uncertainty is relatively low (10–15%), the tracer gas method had been used as a reference method in previous studies (Calvet et al., 2013; Wood et al., 2015). However, the in-situ tracer gas method has many limitations. For the in-situ experiment, delicate injection and uniform distribution of tracer gas are needed. When natural gas such as carbon dioxide is applied, the generation rate of tracer gas is a potential source of error. Furthermore, it has been reported that error levels up to 40% can occur depending on the measuring location of the tracer gas (Zhang et al., 2010). In order to overcome these problems, studies on aerodynamic and ventilation characteristic by combining tracer gas method and CFD have been carried out. Seo et al. (2006; 2009) estimated local ventilation rate inside a naturally ventilated broiler house through CFD simulation. Pawar et al. (2007) analyzed disease diffusion by CFD simulating the diffusion of ammonia near a poultry house. Mostafa et al. (2012) simulated ventilation systems of broiler houses for preventing an inflow of cold external air. The internal local ventilation rate was evaluated by combining CFD simulation and tracer gas methods. Rojano et al. (2015) evaluated ventilation rate of naturally ventilated broiler house using virtual tracer gas and CFD models, which were validated by measured temperature and absolute humidity. However, previous studies have not been able to simulate the change of ventilation rate according to the operating condition of the facility by setting airflow of the exhaust fan to a fixed value. Mostafa et al. (2012) and Kwon et al. (2015) set airflow of exhaust fan in a mechanically ventilated broiler house as the design maximum

airflow of a target fan. Kwon et al. (2016) measured airflow of a fan installed in a swine house according to the power consumption and applied the CFD model. However, there may have been an error in the model as inlet opening area and static pressure were not considered.

2.2. Evaluation of ventilation rate according to static pressure difference

The ventilating operation of a broiler house is based on the design maximum capacity of the exhaust fan in general. Some previous studies have estimated ventilation rate based on the maximum airflow of the exhaust fan too. Knížatová et al. (2010) calculated ventilation rate of broiler house as the product of maximum airflow of tunnel fan and ratio of operating time. Roumeliotis et al. (2010) monitored power consumption and estimated ventilation rate by the ratio of the power consumption for evaluating emission of hazardous gas and dust. However, the ventilation rate through exhaust fan and slot opening of mechanically ventilated broiler houses is complexly affected by the number of operating fans and slot opening area. Thus, analysis with a fixed airflow of exhaust fan has a risk of overestimating the ventilation rate.

The change in airflow through exhaust fan can be predicted by the fan performance curve. The fan performance curve represents the relationship between airflow and static pressure difference of the fan, and its measurement method is specified in ANSI/AMCA 210 and KSB 6311. ANSI/AMCA 210 regulates the dimensions and location of measuring instruments according to the types of inlet and outlet. The method applicable to the free inlet and free outlet corresponding to the fan installed in a livestock house is the outlet chamber. The cross-sectional area of outlet chamber has to be at least 9 times the area of fan outlet, which makes it difficult to apply to an in-situ experiment. Studies that evaluated fan performance in the field have applied various simplified methods, including FANS.

A number of studies using FANS have been carried out on broiler houses and reported decreased in-situ fan performance compared to the design fan performance curve provided by the manufacturer (Li et al., 2005; Gates et al., 2005; Casey et al., 2008). Xin et al. (2009) measured the fan performance curve of exhaust fan in broiler house by FANS and compared with measuring CO_2 concentration to present optimal procedure of the CO_2 balance method. Lin et al. (2011) conducted long-term monitoring of a broiler house's ventilation rate by fan performance curve measured with FANS and monitoring rotation speed of the fan. Morello et al. (2014) measured fan performance curves of tunnel fans in broiler houses using FANS and reported measured fan performance curves were affected

by the operation of fans near the target fan. The airflow of target fan varies 12.6% ± 4.4% at the same static pressure difference according to the fan operating conditions and install location of FANS.

FANS has been reported to have the highest accuracy in the in-situ airflow measurement of fans (Calvet et al., 2013), but had not been commonly used due to its complicated structure. As a simplified airflow measurement device, Pitot tube and hot-wire anemometer have been also applied in multiple studies. Harvey & Belle (2016) measured airflow distribution of axial fan by Pitot traverse for evaluating fan performance. Liang et al. (2016) evaluated fan performance curve of exhaust fan in a broiler house using both multiport averaging Pitot tube (MAPT) system and FANS. As a result, in-situ measurement results with MAPT and FANS had a high agreement of error less than 9%, and in-situ fan performance degraded compared to the design fan performance curve measured according to the ANSI/AMCA 210.

In order to measure the fan performance, static pressure has to be controlled by adjusting opening rate or operating an auxiliary fan. However, measurement according to the structural change in field experiments is laborious and time-consuming. A simplified method for measuring in-situ fan performance curve had been proposed to overcome the problem. Liu et al. (2003) studied the shift of fan performance curve due to the change in rotation speed and surrounding structure of fan and suggested calibrating the in-situ fan performance curve by single in-situ measurement and manufacturers design fan performance curve. Furthermore, Liu et al. (2005) proposed a method calibrating fan performance curve after measuring at low rotational speed, taking into account the difficulty of airflow measurement at high rotational speed in the field. From the comparison of the calibrating method with a single measurement and measured results with various conditions, the coefficient of variation of the RMSD was calculated to be 4.7% (Liu & Liu, 2012). However, the calibrating method suggested by Liu et al. (2003) only considers pressure loss caused by friction. It does not reflect the pressure difference caused by the structural change and measuring point in a free inlet and free outlet type facility such as a livestock house.

The airflow through slot opening can be estimated by the orifice equation. The orifice equation is the relation between the airflow and the static pressure difference of the opening. In order to predict the airflow through the orifice equation, the opening area and discharge coefficient are needed. In contrast to the large number of studies on the fan performance curve in livestock house, there is lack of research on the evaluation of orifice equation and discharge coefficient. Albright (1976) conducted a wind tunnel experiment for evaluating ventilation characteristics of the baffle slotted inlet, which is commonly used in livestock

houses, including broiler and pig house. Discharge coefficient varied 0.721–0.862 according to the opening angle of the baffle, but a tendency was not observed with the angle. The weak negative correlation between the discharge coefficient and the Reynolds number was analyzed. Bottcher et al. (1992) derived a formula for estimating ventilation rate of mechanically ventilated broiler house with a continuous slot opening and assuming discharge coefficient as 0.6 and 1.0. Pearson & Owen (1994) measured discharge coefficient of cladding materials and open ridge of livestock house by wind tunnel experiments. Other studies on layer houses (Timmons et al., 1986), rabbit houses (Hatem et al., 2011), and dairy buildings (Kiwan et al., 2013) have assumed a constant discharge coefficient as a commonly used reference value. However, since the discharge coefficient varies with area and shape of the opening (Heiselberg & Sandberg, 2006), in-situ measurement has to be conducted to accurately estimate the inlet airflow. Wu (2009) designed a dynamic model for simulating the environment of a mechanically ventilated broiler house. The discharge coefficient of the inlet was measured according to the opening area, but not presented in the paper, and applied as a fixed value to simplify the model.

Chapter 3. Materials and Methods

3.1. Experimental broiler house

3.1.1. Ire broiler farm

A broiler farm for environmental monitoring is the Ire broiler farm located in Buyeo, Chungcheongnam-do. The second broiler house on the upper side is selected as the target broiler house in the present study. The dimensions of the target broiler house are as follow: 60 m in length, 15 m in width, 5 m in ridge height, and 3 m in eave height. Fig. 1 and Fig. 2 show the appearance of the Ire farm.

Fig. 1 External view of the Ire broiler farm

Fig. 2 Internal view of target broiler house in Ire broiler farm

The target facility follows a typical mechanical ventilation system. Cross ventilation using sidewall fans and slot openings is applied in winter, and tunnel ventilation using tunnel fans and slot openings or cooling pads is applied in summer. It has three sidewall fans (Euroemme EM36; Munters, Sweden) with diameter 0.915 m and maximum airflow 17,900 CMH on the left wall. Total 10 tunnel fans (Euroemme EM50; Munters, Sweden) with diameter 1.270 m and maximum are located on the back wall. Slot openings (0.6 × 0.2 m) were located with 26 on the left wall and 30 on the right wall. Cooling pads (24 × 1.1 m) are located on each side wall, near the entrance. Four heaters (PW-100A/B, Samsung Inc. Co., Korea) with capacity 70,000 kcal/h are used for heating in winter. Eight circulation fans (450 mm × 450 mm) are installed at a height of 3.4 m to improve the uniformity of the environment.

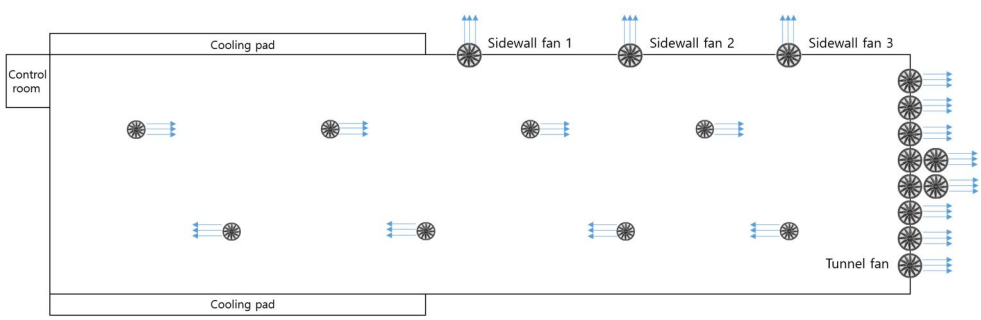

Fig. 3 Schematic diagram of experimental broiler house

All of the facilities are automatically controlled by the farm controlling system (Farm Premium P; Munters, Sweden). The internal environment is monitored by four temperature sensors and one relative humidity sensor. The external environment is also monitored. Ventilation level is controlled by operation cycle of exhaust fans based on the deviation between internal and optimal air temperature. The operation cycles of exhaust fans according to the temperature deviation are shown in Table 1. Operating conditions such as ventilation level, optimum air temperature, and static pressure difference are monitored by the farm controlling software.

Table 1 Fan operation cycle according to ventilation level

Ventilation level	Cycle (sec)		Number of operating fans (No. of continuously operating fans)	
	on	off	Side fan	Tunnel fan
1	10	290	3	0
2	15	285	3	0
3	22	278	3	0
4	37	363	3	0
5	41	259	3	0
⋮				
25	(Continuous)		0	5
26	(Continuous)		0	6
27	(Continuous)		0	7
28	(Continuous)		0	8
29	(Continuous)		0	9
30	(Continuous)		0	10

3.1.2. Daeseon broiler farm

Fig. 4 Aerial photograph of Daeseon broiler farm

Fig. 5 Experimental Daeseon broiler farm

Field experiment for measuring fan performance was conducted on the Daeseon farm which is located on Gimje, Jeollabuk-do. Three mechanically ventilated broiler houses are located on Daeson farm, raising roughly 100,000

heads in total. The experiment was conducted in the first broiler house, which is closest to the entrance. The dimension of the target broiler house is 123 m in length, 15 m in width, 5.5 m in ridge height, and 3.5 m in eave height. Daeseon broiler farm follows a typical mechanical ventilation system, as Ire farm. In winter, cross ventilation using sidewall fans and slot openings is applied. Tunnel ventilation using tunnel fans and slot openings or cooling pads is applied in summer. Exhaust fans of the same model as the Ire farm are used in Daeseon farm. Four sidewall fans (Euroemme EM36; Munters, Sweden) are installed on the left wall and 14 tunnel fans (Euroemme EM50; Munters, Sweden) are installed in the back wall. On each side wall, 41 slot openings are located. Slot openings are 1.13 m long and 0.34 m high. The door of each slot opening is curved and maintains a constant angle of inlet flow regardless of inlet area. Cooling pads (30 m length × height of 1.5 m) are located on each side wall near the entrance. Tunnel doors installed for opening the cooling pads are 30 m long and 1 m height. A windbreak is installed to prevent dust and odor from spreading to neighboring houses. The windbreak is located 3–4 m ahead of the tunnel fans.

Fig. 6 Control system in Daeseon broiler farm

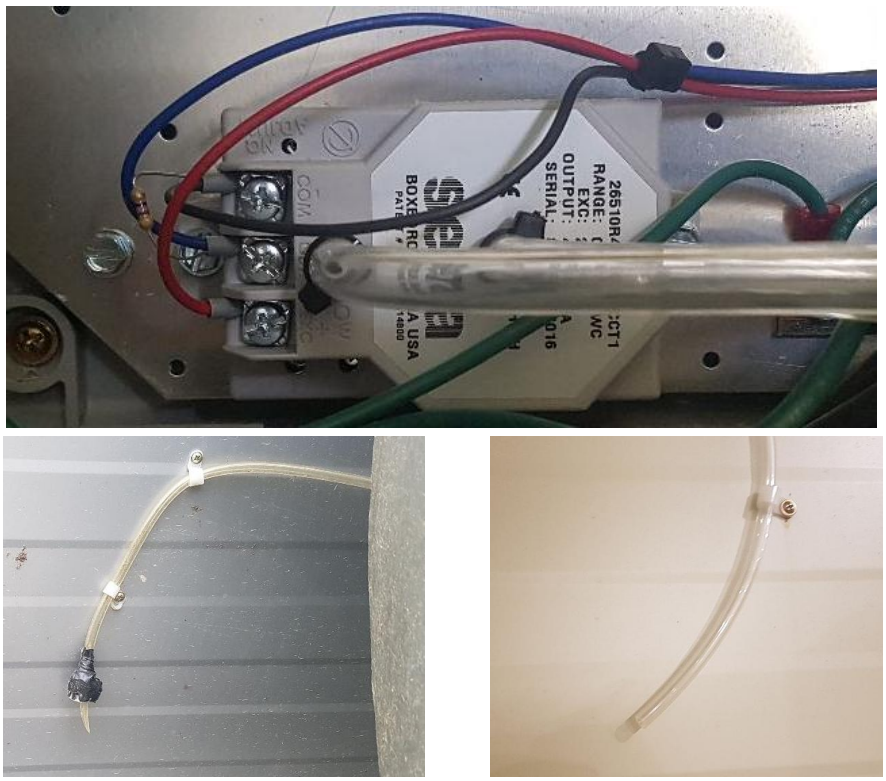

Fig. 7 Differential pressure transducer installed in Daeseon broiler farm

The internal environment of the target broiler house is controlled by an automatic controlling system named Chore-Tronics 2 Controls (Chore-Time, A Division of CTB, Inc., USA) The automatic controlling system included sensors for air temperature, relative humidity, static pressure, and software for automatic control. Sidewall fans and tunnel fans are controlled automatically based on air temperature setting. The individual exhaust fan can be controlled manually if necessary. Slot openings are controlled based on the static pressure difference between inside and outside of broiler house. The static pressure sensor installed in target broiler house was Setra model 265 (Setra Systems, Inc., USA). All slot openings are controlled simultaneously for changing opening area, and cannot be controlled individually. The controlling system and the static pressure sensor are shown in Fig. 6 and Fig. 7.

3.2. Fan performance curve

A fan is a device for creating airflow by rotating impeller and the capacity of the fan is evaluated by the airflow of the inlet. Generally, the capacity of the fan is evaluated by maximum airflow. However, airflow at field decreases depending on

the static pressure difference between inlet and outlet, and characteristics of the surrounding structure, such as duct and damper.

When operating a fan, dynamic pressure of airflow is the same at the inlet and outlet, whereas static pressure is higher at the outlet than at the inlet. The static pressure difference represents the resistance of the airflow due to the surrounding structure. As resistance increase by the structural change, the static pressure difference increases and airflow decreases. A fan performance curve represents the relationship between airflow and static pressure difference of the fan. The fan performance curve shows inherent characteristics of individual fans that are constant in shape, power consumption, and rotation speed. The standard test method of a fan performance curve is specified by KSB 6311 and ANSI/AMCA 210. The manufacturer of a fan generally provides the design fan performance curve, evaluated according to the standard.

Fan performance curve at maximum rotation speed can be approximated by second-order polynomial of airflow and static pressure difference:

$$\Delta P = c_0 + c_1 Q + c_2 Q^2$$

Where, ΔP is the static pressure difference between inlet and outlet of fan (Pa), Q is the airflow of fan (m s^{-1}), c_0, c_1, and c_2 are the coefficients of the fan performance curve.

Design fan performance curve is for the fan performance in standard air condition (Air at 20℃, 50% relative humidity and 101.325 kPa barometric pressure) (ANSI/AMCA 210). For accurate estimation of airflow in the field, airflow should be corrected using field air density by the following equation (Liu & Liu. 2012).

$$\Delta P = \frac{\rho}{\rho_d}(c_0 + c_1 Q + c_2 Q^2)$$

Where, ρ is the standard air density (kg m^{-3}), ρ_d is the field air density (kg m^{-3}).

The performance of fan degrades compared to the design performance for various reasons such as accumulation of dust, aging of the belt, and structural obstacles. Static pressure drop by structural obstacles can be calculated by Darcy equation.

$$P_{loss} = f \cdot \frac{\rho}{2D} \cdot v^2$$
$$P_{loss} \propto v^2 \propto Q^2$$

Where, f is the friction factor (dimensionless), ρ is the air density (kg m□³), D is the hydraulic diameter (m), and v is the mean velocity of fluid (m s□¹).

According to the equation, the pressure drop is proportional to the square of the airflow; therefore, in-situ fan performance curve changes as follows (Liu & Liu, 2012):

$$\Delta P' = \Delta P - P_{loss}$$
$$= c_0 + c_1 Q + c_2 Q^2 - C \cdot Q^2$$

Where, ΔP is the static pressure difference of design fan performance curve (Pa), $\Delta P'$ is the static pressure difference of in-situ fan performance curve (Pa), and C is the coefficient determined by the structural factors.

3.2. Orifice equation

The orifice equation is the commonly used formula for estimating the volumetric flow of fluid through the opening. The orifice equation can be derived through Bernoulli's equation under the assumption of incompressible steady flow (Karava et al., 2004). When sectional area changes by sharp-edged orifice, as in Fig. 8, the following equations are established by Bernoulli's equation and continuity equation, respectively:

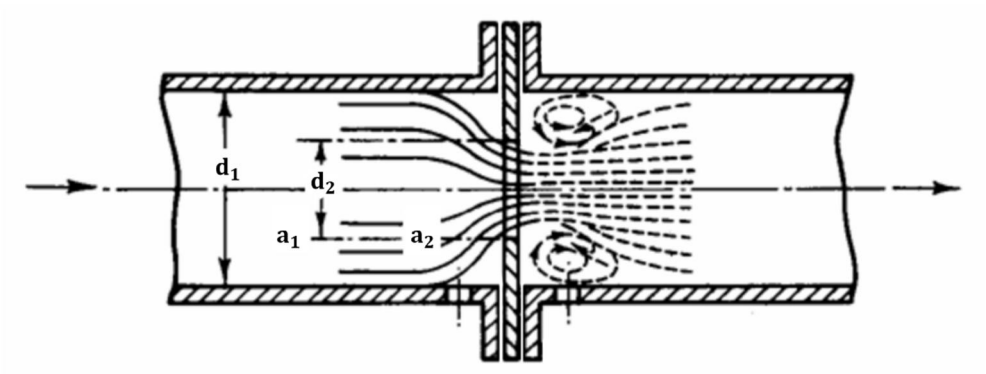

Fig. 8 Flow through an orifice (Ower & Panckhurst, 1977)

$$\frac{1}{2}\rho v_1^2 + p_1 = \frac{1}{2}\rho v_2^2 + p_2$$
$$Q = A_1 \times v_1 = A_2 \times v_2$$

Where, ρ is the density of fluid (kg m□³), v_i is the velocity of fluid in

section i (m s□¹), p_i pi is the static pressure in section i (Pa), A_i is the area of section i (m²), Q is the volumetric flow rate (m³ s□¹).

The velocity and volumetric flow rate of the fluid can be calculated by solving these two equations.

$$v_2 = \sqrt{\frac{2 \times (p_1 - p_2)}{\rho \times \{1 - (A_2/A_1)^2\}}}$$

$$\mathrm{Q} = \mathrm{A}_2 \times v_2 = A_2 \times \sqrt{\frac{2 \times (p_1 - p_2)}{\rho \times \{1 - (A_2/A_1)^2\}}}$$

The fluid through orifice experiences energy losses due to constriction, friction, and turbulence. In order to correct the energy loss, concentration coefficient ($\mathrm{C_c}$) and friction coefficient ($\mathrm{C_f}$) should be applied (Heiselberg & Sandberg, 2006).

$$\mathrm{Q} = \mathrm{C_f} C_c A_2 \sqrt{\frac{2 \times (p_1 - p_2)}{\rho \times \{1 - C_c^2 \times (A_2/A_1)^2\}}}$$

Applying the discharge coefficient ($\mathrm{C_D}$) for simplification of the formula, the flow rate can be estimated by the following equation:

$$\mathrm{Q} = \mathrm{C_D} \times A \times \sqrt{\frac{2 \times \Delta P}{\rho}}$$

$$\mathrm{C_D} = \frac{C_f \times C_c}{\sqrt{1 - C_c^2 \times (A_2/A_1)^2}}$$

Where, ΔP is the static pressure difference between two section (Pa).

Discharge coefficient is generally estimated to be 0.6–0.65 for a square opening (American Society of Heating, Refrigerating Air-Conditioning Engineers, 2001), and 0.9–0.95 for a circular opening (Andersen, 2002). However, discharge coefficient varies with numerous factors, such as shape and roughness of the opening, flow rate, density, and viscosity of fluid (Ower & Panckhurst, 1977). Reynolds number (Re) also affects the discharge coefficient when the flow through the ventilation opening is not fully developed (Karava et al., 2004). Therefore, a field-measured discharge coefficient should be applied rather than the reference value for accurate estimation of flow. Studies are being conducted to evaluate

discharge coefficient according to the shape, area of opening and Reynolds number and so on.

3.3. Experimental instruments

Airflow through exhaust fans was measured by airflow station (manufactured by this research team) and manometer (DP-CALC Micromanometer 5815; TSI Inc., USA). Airflow station is a circular duct with a diameter of 1 m and length of 0.5 m. Pitot tubes are located on traverse plane for measuring dynamic pressure. The number and location of Pitot tubes were in accordance with ANSI/AMCA Standard 210. The dynamic pressure on traverse plane is measured as the difference between total pressure and static pressure and converted to the airflow. The specification of the manometer is shown in Table 2. Temperature and humidity data logger (HOBO UX100-003; Onset Computer Co., USA) was used for monitoring the environment during the experiment. Table 3 shows the specification of the temperature and humidity data logger. The instruments used in the experiments are shown in Fig. 9.

Table 2 Technical specifications of manometer (DP-CALC Micromanometer 5815; TSI Inc., USA)

	Differential pressure	Air velocity
Range	-3735 to 3735 Pa	1.27 to 78.7 m/s
Accuracy	±1 Pa	±1.5% (at 10.2 m/s)
Resolution	0.1 Pa	0.1 m/s

Table 3 Technical specifications of temperature and humidity data logger (HOBO UX100-003; Onset Computer Co., USA)

	Temperature	Relative humidity
Range	-20 to 70℃	15 to 95%
Accuracy	±0.21℃	±3.5%
Resolution	0.024℃	0.07%

(a) Air flow station

(b) DP-CALC Micromanometer 5815

(c) HOBO UX100-003

Fig. 9 Instruments for measuring air flow and velocity

The static pressure difference between inside and outside of Daeseon broiler farm was measured using Setra model 265, which is installed near the control room. The static pressure sensor is linked to the controlling system (Chore-Tronics 2 Controls) in the control room. Hoses were installed for both internal and external walls for measuring the static pressure difference between them. The following Table 4 shows the specification of the sensor.

Table 4 Technical specifications of differential pressure transducer (Setra model 265; Setra Systems, Inc., USA)

Range	0-99.6 Pa (0-0.4 inches of water)
Resolution	2.49 Pa (0.01 inches of water)
Accuracy	±1.0% (full scale)
Compensated temperature range	-18 to 65℃

3.4. Computational Fluid Dynamics (CFD)

CFD is a branch of fluid mechanics that numerically analyzes the behavior of fluid using a computer. The numerical solution is obtained through the Navier–Stokes equation discretized by finite volume method. The numerical analysis process through CFD can be divided into pre-processing, main module, and post-processing. In pre-processing, the geometry and mesh of target model are designed. The flow of the fluid in target model is numerically analyzed by the main module. The result of the main module is analyzed through the post-processing step. Both quantitative and qualitative analyses are possible by deriving numerical value and visualization. A complicated model design and validation process is required for

accurate CFD simulation. However, CFD is applied in various fields due to the efficient simulation and analysis of the result of diverse conditions.

In the main module, non-linear partial differential equations derived by the following formulas are used for analyzing the behavior of the fluid (Fluent, 2009).

Equation for the conservation of mass:

$$\frac{\partial \rho}{\partial t} + \nabla(\rho \vec{u}) = S_m$$

Equation for the conservation of momentum:

$$\frac{\partial}{\partial t}(\rho \vec{u}) + \nabla(\rho \vec{u}\vec{u}) = -\nabla P + \nabla(\vec{\tau}) + \rho \vec{g} + \vec{F}$$

Equation for the conservation of energy:

$$\frac{\partial}{\partial t}(\rho E) + \nabla\big(\vec{v}(\rho E + P)\big) = \nabla\left(K_{eff}\nabla T - \sum h\vec{J} + \left(\vec{\tau}_{eff}\vec{u}\right)\right) + S_{\mathrm{h}}$$

Where ρ is the density (kg m^{-3}), $\vec{u}$ is the velocity (m s^{-1}), P is the static pressure (Pa), S_m is the mass added to the continuous phase from the dispersed second phase (kg m^{-3}), $\vec{\tau}$ is the stress tensor (kg m^{-1} s^{-2}), $\vec{g}$ is gravitational acceleration (m s^{-2}), $\vec{F}$ is the external body force (kg m s^{-2}), E is the total energy (kg m^2 s^{-2} kg^{-1}), K_{eff} is the effective conductivity (kg m^{-1} s^3 K), T is the temperature (K), $\vec{\tau}_{eff}$ is the effective stress tensor (kg m^{-1} s^{-2}), and S_{h} includes the heat of chemical reaction and any other volumetric heat sources (kg m^{-1} s^3).

This study used ANSYS DesignModeler and Meshing (Release 16.1, ANSYS Inc., USA) for design of model geometry and mesh, and ANSYS Fluent (Release 16.1, ANSYS Inc., USA) for the main module.

3.5. Research method

3.5.1. Measurement of ventilation rate of Ire broiler house in winter condition

Airflow measurement of the exhaust fan in winter ventilating condition was conducted on November 11, 2016. Airflow of three sidewall fans was measured according to the number of operating fans using the airflow station and manometer (DP-CALC Micromanometer 5815). The controller in the target facility controls the first sidewall fan (SF1 on Fig. 3) independently, and the other two sidewall fans (SF2, SF3) simultaneously. Accordingly, the experiment was conducted on three

operating conditions: operating one (SF1), two (SF2, SF3), and three sidewall fans (SF1, SF2, SF3). Airflow of each sidewall fan was measured for evaluating airflow decrease in the winter slot opening condition.

the airflow station was connected to the outlet of target sidewall fan with a 1-m-long fabric duct. Dynamic pressure at the airflow station was measured by manometer. For each experimental condition, the dynamic pressure was measured three times repeatedly after stabilization of the air flow for 15 minutes. The opening height of all slot openings was 5 cm, which is the typical winter inlet condition of the target broiler house. For maintaining constant static pressure difference, all other vents were closed during the experiment.

Fig. 10 Measuring air flow of sidewall fan

3.5.2. Measurement of ventilation characteristics in Daeseon broiler farm

The experiment in the Daeseon broiler farm was conducted on September 27-28, 2017, for evaluating in-situ fan performance curve and discharge coefficient. The experiment was conducted at the resting period of the target broiler house between breeding periods (flocks). Thus, the target broiler house was empty and obstacles to the air flow did not exist, including broiler and bedding material.

Airflow was measured at one tunnel fan at the bottom center among the 14 tunnel fans. An airflow station manufactured by this research team was installed for airflow measurement. Fabric duct (1.5 m long) connected the airflow station and outlet of the target tunnel fan. Dynamic pressure at the airflow station was measured by Pitot tube inside the airflow station and manometer. Air temperature and relative humidity were monitored simultaneously at 5-minute intervals, using HOBO UX100-003. The atmospheric pressure of AWS (Automatic Weather System) data provided by Korea Meteorological Administration were used for calculating air density. Air density was calculated by the following equation:

$$\rho = \frac{p_b - 0.378 \times p_p}{R \times t_d}$$

Where, ρ is the air density (kg m^{-3}), p_b is atmospheric pressure (Pa), p_p is the vapor partial pressure (Pa), R is the gas constant (287 J kg^{-1} K^{-1}), and t_d is the dry bulb temperature (℃).

The entrance and tunnel doors of cooling pads were closed during the experiment for maintaining airflow and static pressure difference. For controlling static pressure difference between inside and outside of target broiler house, number of operating tunnel fans (1, 2, 4, 6, 8, 10, 12, and 14) and opening height of slot openings (0.05, 0.10, 0.15, 0.2, and 0.34 m) were adjusted (Fig. 11, Fig. 12). Static pressure difference was measured by the sensor (Setra model 265), which is used for the operation of the target broiler house.

(a) Operating target tunnel fan (b) Operating all tunnel fans

Fig. 11 Controlling the number of operating tunnel fans

(a) Height 0.05 m

(b) Height 0.10 m

(c) Height 0.15 m

(d) Height 0.20 m

(e) Height 0.34 m

Fig. 12 Controlling slot opening height

In order to prevent the damage to the facility due to the excessive static pressure difference, measurements were conducted with cases that static pressure difference was expected to be under 40 Pa (0.16 inches of water). Static pressure difference was estimated before the experiment, by design fan performance curve of target tunnel fan and orifice equation. The discharge coefficient for orifice equation was estimated to be 0.65. Fig. 13 is an example of airflow and static pressure difference estimation when four tunnel fans are operated. Opening height was 5 cm, which estimated that static pressure difference exceeding 40 Pa was excluded from experimental cases. The selected experimental cases are shown in Table 5. The locations of operating tunnel fans were decided symmetrically, according to the number of operating fans (Fig. 14).

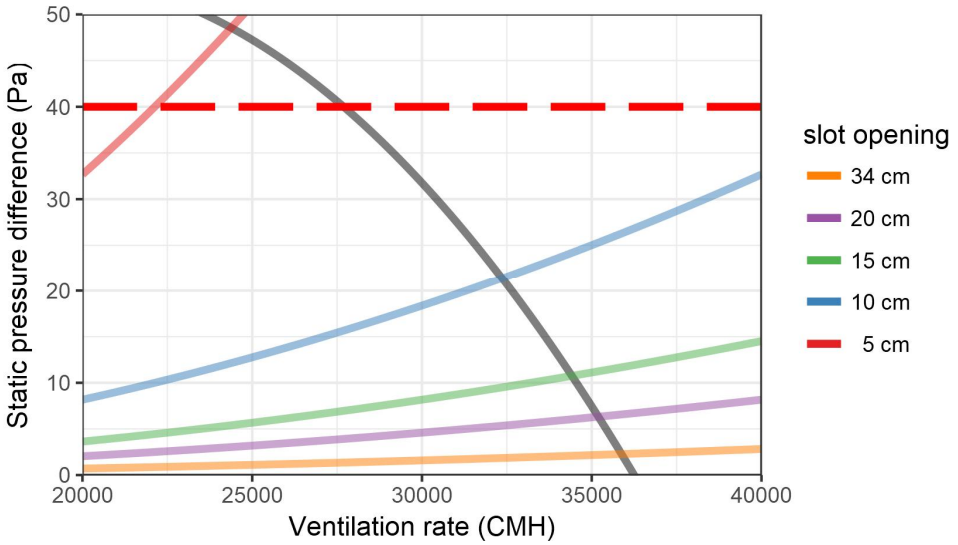

Fig. 13 Estimated airflow and static pressure according to the slot opening area when 4 fans are operated

Table 5 Experimental cases of airflow measurement of tunnel fan

Slot opening height (opening rate)	Number of operating tunnel fans
34 cm (100%)	1, 2, 4, 6, 8, 10, 12, 14
20 cm (55.8%)	1, 2, 4, 6, 8, 10, 12
15 cm (44.1%)	1, 2, 4, 6, 8
10 cm (29.4%)	1, 2, 4, 6
5 cm (14.7%)	1, 2, 4

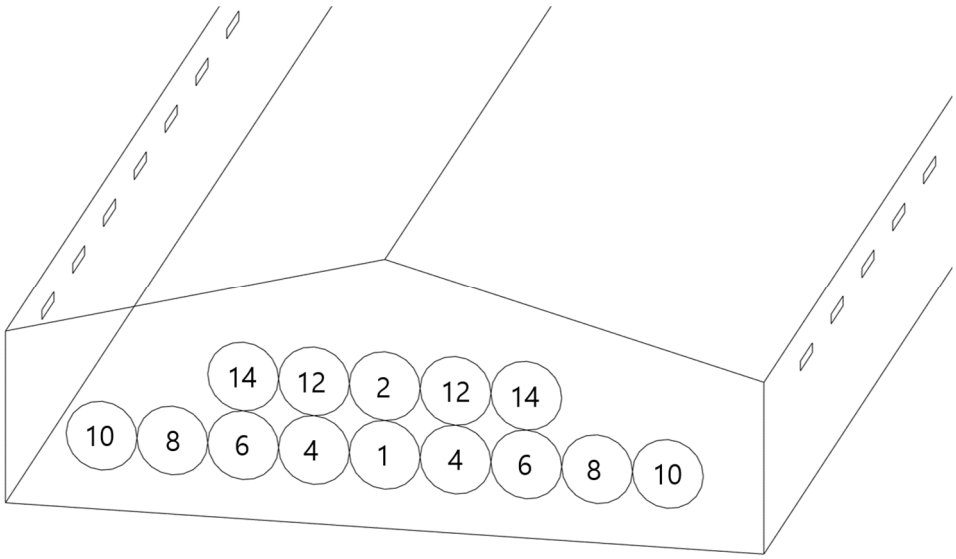

Fig. 14 Location of operating tunnel fans according to the total number of operating fans

For evaluating the effect of the windbreak on the performance of the tunnel fan, the experiment was conducted in with and without windbreak conditions (Fig. 15). Stabilization of air flow was carried out for 15 minutes for each experimental conditions. After stabilization, airflow was measured three times for each condition. Each measurement was conducted for 1 minute. The experiment was suspended when external wind speed was high to prevent interference due to dynamic pressure to the measurement of static pressure.

(a) Airflow measurement without windbreak

(b) Airflow measurement with windbreak

Fig. 15 Airflow measurement according to the presence of windbreak

3.5.3. Ventilation rate formula according to operating condition

Formula for evaluating ventilation rate of mechanically ventilated broiler house was derived from in-situ fan performance curve and orifice equation. Assuming the constant air density, the airflow through exhaust fan is equal to airflow through the slot opening by continuity equation. Airflow through exhaust fan and slot opening can be estimated by fan performance curve and orifice equation, respectively. Therefore, by combining those two equations, ventilation rate (Q) and static pressure difference (ΔP) can be calculated. When the fan performance curve and orifice equation are plotted in the airflow - static pressure relation graph, the point that two curves intersect indicates the ventilation rate and static pressure difference of the facility (Fig. 16).

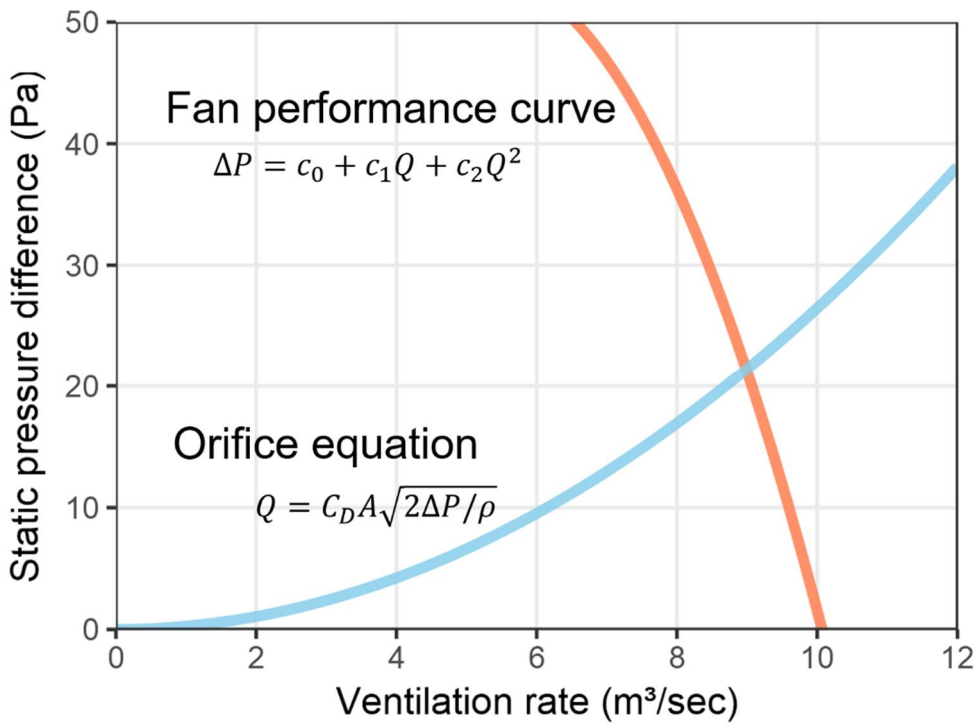

Fig. 16 Estimation of airflow and static pressure by fan performance curve and orifice equation

Method for solving by equations is as follows. Let Q be total ventilation rate of mechanically ventilated facility, and n be number of operating exhaust fans. Assuming the same performance for all fans, the airflow through one exhaust fan is equal to Q/n. Therefore, the fan performance curve is as follows:

$$\Delta P = c_0 + c_1\left(Q/n\right) + c_2\left(Q/n\right)^2$$

The orifice equation can be transformed into a formula for static pressure difference (ΔP) as follows:

$$\Delta P = \frac{\rho}{2C_D^2A^2}Q^2$$

The second order polynomial of airflow can be derived by combining the following two equations:

$$c_0 + \frac{c_1}{n}Q + \left(\frac{c_2}{n^2} - \frac{\rho}{2C_D^2A^2}\right)Q^2 = 0$$

$$c_0 n^2 + c_1 nQ + \left(c_2 - \frac{\rho n^2}{2C_D^2A^2}\right)Q^2 = 0$$

Let c_2' be the coefficient of the square of airflow ($c_2' = c_2 - \rho n^2 C_D^{-2} A^{-2}/2$), then ventilation rate Q can be obtained by solution of second-order equation as follows:

$$Q = \frac{-c_1 + \sqrt{c_1^2 - 4c_0c_2'}}{2c_2'} \times n$$

Therefore, the ventilation rate of mechanically ventilated broiler house according to the number of operating exhaust fans (n) and slot opening area (A) can be estimated using the derived equation.

3.5.4. CFD model design and validation

The CFD model of Daeseon broiler farm was designed for analyzing in-situ fan performance curve and spatial distribution of static pressure. The dimensions of the CFD model are the same as the target broiler house (123 m in length, 15 m in width, 3.5 m in eave height, and 5.5 m in ridge height). Outlets of the model are 14 tunnel fans (Euroemme EM50 Exhaust fan; Munters) located on the back wall, and inlets are slot openings (1.13 m in length and 0.34 m in height) located 41 on each side wall. The tunnel fans are designed with circular surface (diameter 1.4 m) at the same location as the target broiler house (Fig. 17). Slot openings were located on

side walls at regular intervals. CFD models of each experimental slot opening height (0.05, 0.1, 0.15, 0.2, 0.34 m) were designed. Meshes of the models were designed as tetra, pyramid, and hex grid, and total number of meshes were 2.2 to 4.7 million. SST k-ω turbulence model used in the previous researches on livestock facilities was applied (Shen et al., 2012; Li et al., 2016).

Each slot opening was designed to contain at least 3×5 meshes to accurately simulate inlet flow. The complex structure was simplified for the efficiency of the calculation (Fig. 17).

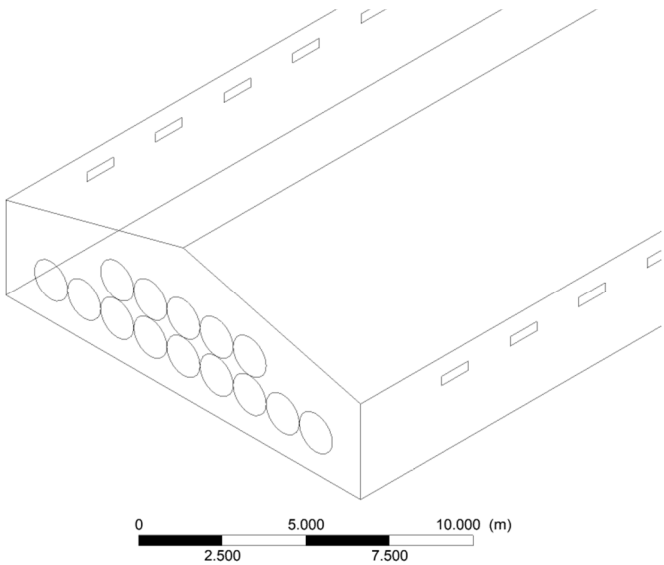

Fig. 17 Geometry of Daeseon broiler farm CFD simulation model

The boundary condition of slot opening was set to inlet-vent for simulating internal and external static pressure difference. Unlike pressure inlet condition, which had been used in previous studies, inlet-vent condition simulates the static pressure difference as follows:

$$\Delta P = k_L \frac{\rho}{2} v^2$$

Where, ΔP is the static pressure difference between the internal and external area of the model (Pa), k_L is the loss coefficient (dimensionless), ρ is the density of fluid (kg m^{-3}), and v is the velocity of inlet flow (m s^{-1}).

Orifice equation also represents the relationship between airflow and static pressure difference, and can be transformed into similar forms. Therefore, loss coefficient (k_L) can be calculated by following equation:

$$Q = C_D A\sqrt{2\Delta P/\rho}$$

$$\Delta P = \frac{1}{C_D^2} \times \frac{\rho}{2} \times \left(\frac{Q}{A}\right)^2 = \frac{1}{C_D^2} \times \frac{\rho}{2} v^2 = k_L \frac{\rho}{2} v^2$$

$$k_L = 1/C_D^2$$

Where, Q is airflow through inlet (m^3 s^{-1}), A is an opening area of the inlet (m^2).

The loss coefficient calculated by measured discharge coefficient was applied to the model according to the slot opening area.

The boundary condition of tunnel fan was set to fan condition. Design fan performance curve provided by the manufacturer was applied (Fig. 18).

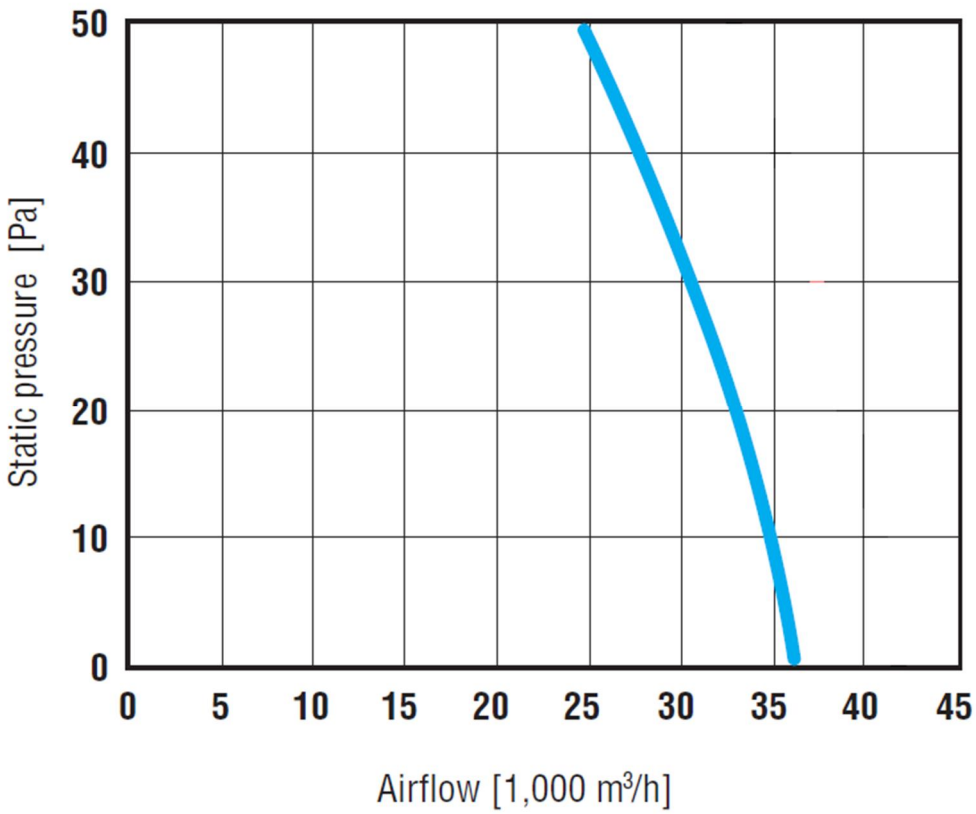

Fig. 18 Design fan performance curve of target tunnel fan

The design fan performance curve was approximated by a second-order polynomial (Liu & Liu, 2012). The fan performance curve was applied as the formula for air velocity and static pressure difference. Design fan performance

curve converted airflow into air velocity is as follows:

$$\Delta P = -7.668 + 36.619 \cdot v - 5.419 \cdot v^2$$

Where, ΔP is the static pressure difference between the inlet and outlet of the fan (Pa), and v is the velocity of outlet flow (m s□¹).

Design fan performance curve of target tunnel fan is provided only in limited range (static pressure difference 0–50 Pa and airflow over 25,000 CMH). In this study, the static pressure difference was assumed to be 50 Pa when airflow is less than 25,000 CMH.

CFD simulation cases with number of operating tunnel fans and slot opening were same as experimental conditions. Simulated airflow of bottom center tunnel fan and distribution of static pressure were analyzed. CFD model was validated by comparing simulated and measured airflow. Regression analysis of the airflow with operating condition (number of operating tunnel fans, slot opening area) and data acquisition method (measured or CFD simulated) was conducted. The p-value of the method was used to test whether significant difference occurred between measured and simulated airflow.

Additionally, three models with different lengths were designed to analyze the change of ventilation characteristics according to the structure of the broiler house. The dimension of standard broiler house published in 2016 is 14 m in width, 3.3 m in eave height, and 5.6 m in ridge height, similar to the experimental broiler house (respectively 15, 3.5, and 5.5 m). On the other hand, the length of the broiler house is changeable within a range of 114.3 m or less. Considering the changeable length of the broiler house, additional CFD models of length 60, 80, and 100 m were designed. Specifications of additional models were same as the original CFD model except the length. Slot openings were designed as fully open condition (0.34×1.13 m) and numbers of slot openings were adjusted according to the length of the model. Fan performance curve of additional CFD models were evaluated by simulation results according to the number of operating tunnel fans (2, 4, 6, 8, 10, 12, or 14). The multiple regression analysis was conducted to determine whether fan performance curve changes with the length of broiler house.

Chapter 4. Results and Discussion

4.1. Ventilation rate measurement in Ire broiler farm

The airflow of sidewall fan in Ire broiler farm was measured in conditions of operating one fan (SF1), two fans (SF2, SF3), and three fans (SF1, SF2, SF3) at the same time. The measurement results are shown in Table 6.

Table 6 Airflow measurement of side fan in Ire broiler farm

No. of operating fans	Target cross fan	Dynamic pressure (Pa)			Airflow (CMH)
1	SF1	18.06	19.14	19.07	18,932
2	SF2	14.47	12.68	14.95	16,376
2	SF3	12.57	11.91	12.18	15,281
3	SF1	7.12	8.66	9.80	12,765
3	SF2	13.47	13.42	12.62	15,864
3	SF3	8.16	8.48	8.71	12,707

The model of all target sidewall fans was Euroemme EM36 (Munters, Sweden), and power consumption of them was set at 0.5 hp. According to the design fan performance curve provided by the manufacturer, the maximum airflow of the target fan is 17,900 CMH when the static pressure difference is 0 Pa. Measured airflow of target sidewall fans decreased as the number of operating fans increased. The average reduction rate compared to the designed maximum airflow was 11.6% when two sidewall fans were operating (SF2, SF3), and 23.0% when all three fans were operating. The ventilation rate of the target broiler house is controlled by operating cycle of exhaust fans, not by the number of operating fans. When cross ventilation is conducted, all three sidewall fans operate simultaneously. Therefore, the actual ventilation rate of target broiler house was calculated as 77.0% of the designed ventilation rate during the winter season. It was analyzed that the ventilation rate decreased due to the narrow slot opening area and excessive static pressure difference. Considering the results of this experiment, it is necessary to evaluate the ventilation rate according to the operating conditions of the mechanically ventilated broiler house.

4.2. Airflow measurement in Daeseon broiler farm

4.2.1. Measurement of environmental factors and ventilation characteristic

The experiment was conducted in the Daeseon broiler farm to evaluate ventilation characteristics. The airflow of tunnel fan and the static pressure difference between inside and outside of the broiler house were measured according to the number of operating fans and slot opening height. The air temperature and relative humidity were monitored simultaneously for calculating air density, which was required to calculate the airflow from dynamic pressure. The average air temperature during the experiment was measured as 22.4℃ (minimum 20.5℃, maximum 25.2℃), relative humidity was 76.4% (56.9%–87.1%), and atmospheric pressure was 999.96 hPa (997.10–1004.00 hPa). The average air density was calculated as 1.1696 kg m□³ (1.1633–1.1761 kg m□³).

Table 6 and Table 7 show the measured airflow of target tunnel fan and static pressure difference. The range of each measurement was indicated according to the number of operating fans and slot opening height.

Table 7 Range of measured airflow and static pressure according to the number of operating tunnel fans

No. of operating fans	Minimum opening height of slot (cm)	Airflow of target fan (CMH)		Static pressure (Pa)	
		Minimum	Maximum	Minimum	Maximum
1	5	25,487	27,409	-2.5	0.0
2	5	24,051	27,237	-2.5	10.0
4	5	23,086	27,572	0.0	32.4
6	10	24,430	27,114	5.0	27.4
8	15	24,230	25,956	12.5	24.9
10	20	23,659	24,540	19.9	27.4
12	20	21,997	22,616	27.4	34.9
14	34	20,222	20,483	37.4	37.4

Table 8 Range of measured airflow and static pressure according to the slot opening size

Slot opening height (cm)	Maximum number of operating fans	Airflow of target fan (CMH)		Static pressure (Pa)	
		Minimum	Maximum	Minimum	Maximum
5	4	23,086	26,346	0.0	32.4
10	6	24,430	26,666	0.0	27.4
15	8	24,230	27,572	0.0	24.9
20	12	21,997	27,409	-2.5	34.9
34	14	20,222	27,455	-2.5	37.4

The static pressure difference was measured as a negative value under some conditions, which means the external static pressure was lower than that inside. As performing mechanical ventilation through the exhaust fan, the static pressure inside the facility is theoretically lower than that outside. Therefore, it is considered that an error occurred due to the dynamic pressure around the tube for static pressure measurement. Negative static pressure difference was measured under condition of fewer than two fans operating and slot opening height was greater than 20 cm. In other words, an error occurred under the condition of low total ventilation rate and static pressure. Therefore, in order to minimize the error, the experiment was conducted with the conditions that the static pressure difference was relatively high. The experiment was suspended while wind blowing outside for preventing error by dynamic pressure.

The designed maximum airflow of target tunnel fan is 36,180 CMH. The measured maximum airflow without windbreak was 27,571 CMH, which is 76.2% of designed maximum airflow. The cause of the airflow decrease can be presumed to be the installation of the shutter to prevent the infiltration, accumulation of dust, and the deterioration of fan. Therefore, in-situ fan performance needs to be evaluated to estimate the exact ventilation rate in the mechanically ventilated broiler house. The minimum airflow of the target tunnel fan was measured when all 14 tunnel fans were operated and slot openings were fully opened. The condition corresponds to the maximum ventilation condition using tunnel fans and slot openings. The minimum airflow of the target fan was 20,222 CMH (55.9% of designed maximum airflow), and the static pressure difference was measured as 37.36 Pa.

4.2.2. Evaluation of in-situ fan performance curve

The in-situ fan performance curve was derived by regression analysis using measured airflow and static pressure difference. The regression analysis was conducted in a second-order polynomial with reference to Liu et al. (2003). The results of regression analysis with all measured data are shown in Table 9.

Table 9 Regression analysis of in-situ fan performance curve with entire measurement data

Multiple R^2	Adjusted R^2	F-statistic	p-value
0.7968	0.7911	141.1	< 2.2e-16
	Estimate	Standard error	p-value
(intercept)	2.529e+01	1.019e+02	0.805
Q	5.742e-03	8.412e-03	0.497
Q^2	-2.459e-07	1.728e-07	0.159

As a result of the analysis, the adjusted R^2 was 0.7296, which was relatively low, and the p-value of all variables was estimated to be over 0.159. The results of the regression analysis were considered to be inadequate, considering the statistics. It was presumed that the reliability of the regression model was low due to the error in conditions when the static pressure difference was relatively low. The error was considered to occurred by external air flow and small resolution of the sensor. When the static pressure difference was measured as 0 Pa, the measured airflow had a high deviation (25,501–27,455 CMH). The regression analysis was performed again with the data of static pressure difference over 10 Pa, in order to improve the accuracy. The result is shown in Table 10.

Table 10 Regression analysis of in-situ fan performance curve without outliers

Multiple R^2	Adjusted R^2	F-statistic	p-value
0.9063	0.9006	159.6	< 2.2e-16
	Estimate	Standard error	p-value
(intercept)	-2.417e+02	8.208e+01	5.891e-03 **
Q	2.784e-02	7.055e-03	3.920e-04 ***
Q^2	-6.959e-07	1.510e-07	5.820e-05 ***

$$\Delta P = -241.7 + 2.784 \cdot 10^{-2} Q - 6.959 \cdot 10^{-7} Q^2$$

Where, ΔP is the static pressure difference between inside and outside of the broiler house (Pa), Q is the airflow through the fan (CMH).

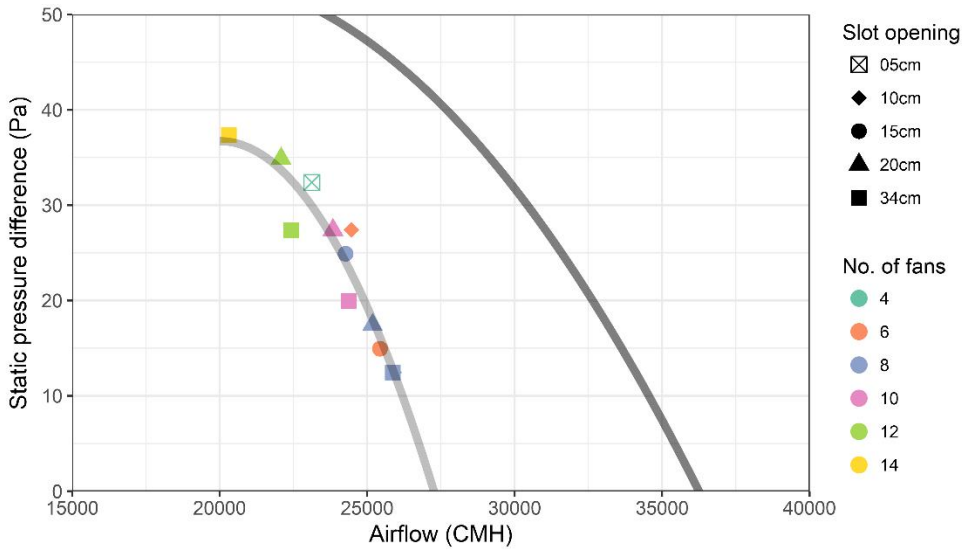

Fig. 19 In-situ and design fan performance curve of target tunnel fan

The R^2 of the improved regression model was calculated as 0.9006. The p-values of all variables were calculated to be less than 0.001, which is considered to have a significant effect on the static pressure difference. The in-situ and design fan performance curves are shown in Fig. 19.

The static pressure difference of in-situ fan performance curve derived from the regression analysis was lower than 20 Pa compared to the manufacturer-provided design fan performance curve. The difference can be caused by the performance degradation by aging and the difference between the standard performance test method and the field measurement environment. Following the standard performance test, the ducts are installed at the inlet and outlet of the target fan. Therefore, static pressure is constant along the ducts and can be easily measured. However, an exhaust fan installed in mechanically ventilated broiler house has a free inlet and free outlet, not ducts. The static pressure in the facility increases as the distance from the exhaust fan increases and the dynamic pressure drops. The static pressure sensor in the target broiler house was installed near the control room, which is a typical installation location for convenience of operation. The static pressure near the control room represents the average static pressure in the facility including slot openings. The measured static pressure difference can be used to calculate the airflow through slot openings. However, it is different from the static pressure difference in the exhaust fans, which is determined by the fan

performance curve. The differences between design and in-situ fan performance curves are considered to be influenced by the distribution of static pressure.

The static pressure difference is formed in the range of 2.5–30 Pa, when the broiler house is tunnel-ventilated (Casey et al., 2008). Under that static pressure range, the ventilation rate calculated by in-situ fan performance curve is 24.1–26.6% lower than the airflow by design fan performance curve. Table 11 shows the airflow reduction rate according to the static pressure difference.

Table 11 Airflow reduction of in-situ fan performance compared to design fan performance

Static pressure (Pa)	Airflow of target tunnel fan (CMH)		Reduction ratio
	Design	In-situ	
0	36,250	27,266	24.8 %
10	34,551	26,199	24.2 %
20	32,645	24,904	23.7 %
30	30,434	23,111	24.1 %

For estimating ventilation rate using design fan performance curve, static pressure difference has to be measured on the exhaust fan. However, the static pressure sensor is practically difficult to be installed on the exhaust fans in terms of accuracy and maintenance problems. Static pressure is difficult to measure near the exhaust fan due to the high dynamic pressure and turbulence intensity. It is also expected that the maintenance of the sensor will be laborious because of the accumulated dust from the broiler house (Fig. 20). Therefore, the in-situ fan performance curve (the relationship between fan airflow and average static pressure difference) measured in this study is more suitable for ventilation rate estimation than the design fan performance curve (the relationship between fan airflow and fan static pressure difference).

Fig. 20 Dust accumulated on blades and shutters of target tunnel fan

4.2.3. Airflow decrease by windbreak

For evaluating the decline of ventilation rate due to the windbreak, the fan performance curve according to the presence of the windbreak was analyzed. The changes of the P–Q relationship with the installation of windbreak was tested by regression analysis. A multiple regression of the static pressure (P) was conducted with a second-order polynomial of fan airflow (Q), with a nominal variable 'windbreak' indicating whether windbreak is installed. The data of static pressure difference over 10 Pa were used as with the previous analysis. The result of multiple regression analysis is shown in Table 12.

Table 12 Regression analysis of static pressure with airflow and windbreak installation

Multiple R^2	Adjusted R^2	F-statistic	p-value
0.8737	0.8676	142.9	< 2.2e-16
	Estimate	Standard error	p-value
(intercept)	8.309e+01	4.370e+01	0.0619 .
Q	-7.526e-04	3.891e-03	0.8473
Q^2	-9.432e-08	8.633e-08	0.2788
Windbreak	1.333e+01	9.769e-01	< 2e-16 ***

As a result, the adjusted R^2 was calculated to be 0.8676, and the regression

model was considered to be significant (p-value < 2.2e-16). The p-value of 'Windbreak', a categorical variable whether windbreak is installed was evaluated to be less than 0.001. Thus, the performance of the target tunnel fan was significantly changed by installing a windbreak.

Regression analysis was performed to evaluate fan performance curve with the windbreak, and the method in detail is the same as the previous regression analysis. The results of regression analysis are indicated in Table 13 and Fig. 21 shows the design and in-situ fan performance curves according to the installation of the windbreak.

Table 13 Regression analysis of in-situ fan performance curve with windbreak

Multiple R^2	Adjusted R^2	F-statistic	p-value
0.9296	0.9244	178.3	2.769e-16
	Estimate	Standard error	p-value
(intercept)	-2.070e+01	8.343e+01	0.8059
Q	1.004e-02	7.945e-03	0.2172
Q^2	-3.710e-07	1.886e-07	0.0595 .

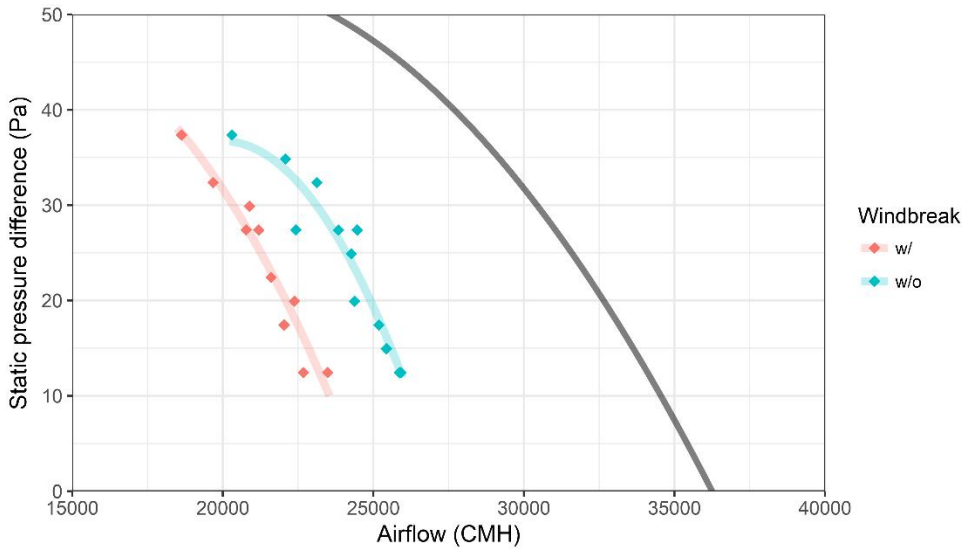

Fig. 21 Design and in-situ fan performance curve according to the installation of windbreak

The airflow was decreased 9.3–12.0% at the typical static pressure difference (2.5–30 Pa) in tunnel ventilation condition due to the windbreak. Compared with the airflow predicted by the manufacturer's design fan performance curve, the

reduction rate was estimated to be 31.6–33.2%. The airflow reduction rate according to the static pressure is as given in Table 14.

Ford and Riskowski (2003) studied the airflow reduction of the agricultural fan by windbreak through the lab experiment. The airflow reduction rate was evaluated according to the static pressure difference and distance of windbreak from the fan. As a result of the experiment under a similar condition of this study (fan diameter 1.4 m, windbreak distance 3.05 m, static pressure difference 0–37 Pa), airflow reduction rate was 9–14%, which is comparable to the result of this study. It was reported in the same study that significant airflow change was not observed when the distance to the windbreak was more than four times the fan diameter (Ford & Riskowski, 2003). Considering the result of previous studies, the windbreak of target broiler house is recommended to be located at a distance of at least 5 m from the tunnel fan.

Table 14 Airflow reduction due to windbreak compared to the design and in-situ fan performance

Static pressure (Pa)	Airflow reduction ratio	
	In-situ fan performance	Design fan performance
0	9.0%	31.6%
10	10.1%	31.9%
20	11.3%	32.3%
30	12.0%	33.2%

4.2.4. Evaluation of discharge coefficient of slot opening

Discharge coefficient was evaluated by regression analysis with static pressure difference and airflow through a slot opening. For the analysis, it was assumed that the static pressure inside the broiler house is uniformly distributed and the airflow of all slot openings identical. The airflow through one slot opening was calculated by dividing the total ventilation rate by the number of slot openings. The discharge coefficient is affected by the geometry of the orifice, and thus by opening area of slot opening. The discharge coefficient for each slot opening size was calculated. Second order polynomial regression model was analyzed according to the orifice equation.

$$\Delta P = \frac{\rho}{2A^2 C_D^2} Q^2 = C \times Q^2$$

Where, ΔP is static pressure difference between inside and outside of the

broiler house (Pa), Q is airflow of slot opening (m^3 s^{-1}), ρ is air density (kg m^{-3}), C_D is discharge coefficient, A is slot opening area (m^2), and C is the coefficient derived from the regression analysis

Discharge coefficient was calculated from the coefficient C and air density and slot opening area at the time of the experiment. The results of regression analysis and discharge coefficient are shown Table 15 and Fig. 22.

Table 15 Result of regression analysis according to slot opening height for evaluating discharge coefficient

Slot opening height (cm)	Coefficient	p-value	Adjusted R^2	Discharge coefficient (C_D)
5	332.660	1.06e-08	0.9988	0.743
10	108.476	5.49e-12	0.9976	0.650
15	55.643	2.28e-09	0.9893	0.605
20	41.457	< 2e-16	0.9960	0.526
34	33.473	9.75e-12	0.9643	0.344

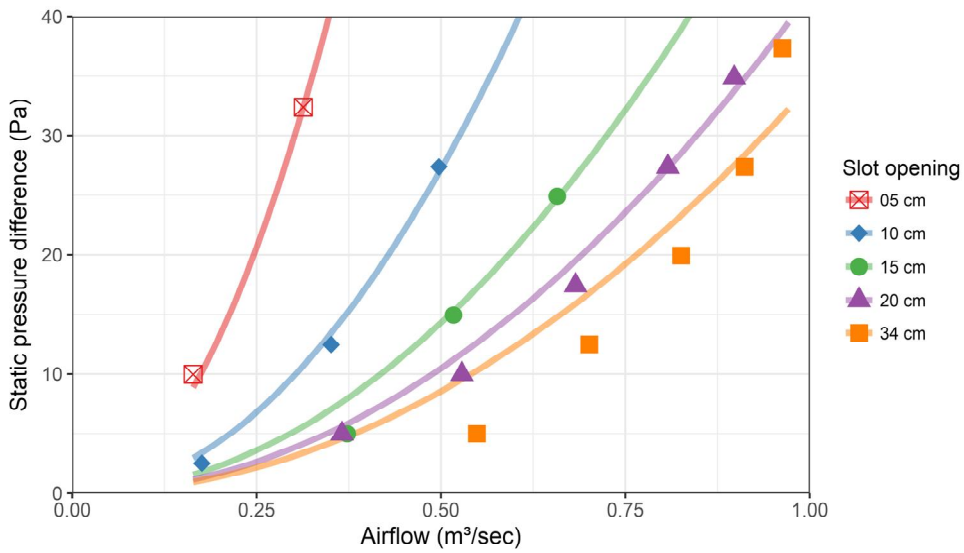

Fig. 22 Regression analysis of static pressure difference with airflow of slot opening according to slot opening height

Regression analysis showed that the coefficient of the square of airflow had a significant effect on the static pressure difference for all slot opening areas. The regression results were considered appropriate, as the adjusted R^2 was calculated to

be over 0.96 for all slot opening area. The discharge coefficient decreased as the slot opening area increase, and this tendency is consistent with the previous study on bottom-hung windows. Bottom-hung windows are similar in structure to the slot opening used in broiler houses. The bottom part is fixed to the wall, and the opening area is adjusted by the angle. Heiselberg and Sandberg (2006) found that the discharge coefficient of bottom-hung window tended to decrease with increasing opening area (Fig. 23).

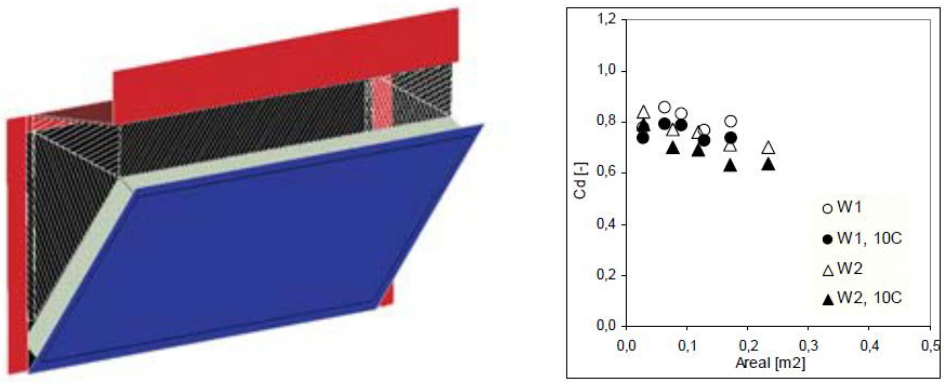

(a) Schematic diagram

(b) Discharge coefficient according to the opening area

Fig. 23 Schematic diagram and discharge coefficient according to the opening area of bottom-hung window (Heiselberg & Sandberg, 2006)

Regression analysis on the discharge coefficient was conducted for analyzing trend and general application. The slot opening area and Reynolds number were used for linear regression analysis. The linear regression analysis results of the discharge coefficient to the slot opening area are shown in Table 16 and Fig. 24.

Table 16 Regression analysis of discharge coefficient with slot opening area

Multiple R^2	Adjusted R^2	F-statistic	p-value
0.8540	0.8512	304.2	< 2.2e-16
	Estimate	Standard error	p-value
(intercept)	0.80867	0.01592	< 2e-16 ***
Slot opening area (m^2)	-1.11129	0.06372	< 2e-16 ***

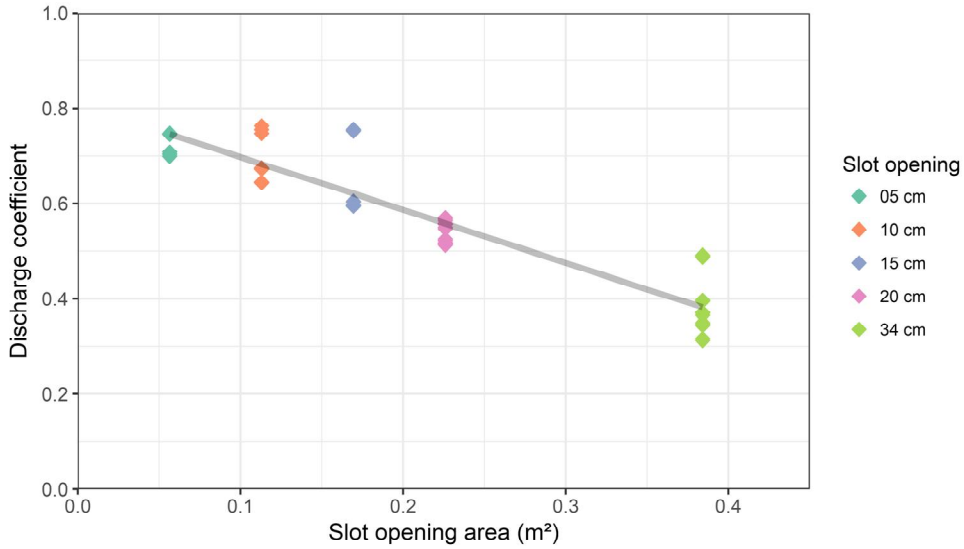

Fig. 24 Regression analysis of discharge coefficient with slot opening area

The discharge coefficient was significantly decreased (p-value < 2e-16) by the slot opening area. The adjusted R^2 of the model was 0.8512, which indicates that the regression model is reliable.

Reynolds number (Re) is dimensionless quantity used in fluid mechanics which can distinguish between laminar and turbulent flow. Previous studies have reported a change in the discharge coefficient according to Reynolds number, even in fully developed turbulence regions that Reynolds number exceeds 2000 (True et al., 2003; Karava et al., 2004). Reynolds number is calculated by following formula:

$$\mathrm{Re} = \frac{\rho v L}{\mu} = \frac{v L}{\nu}$$

Where, v is the velocity of the fluid (m s□¹), L is the characteristic linear dimension, ρ is density (kg m□³), μ is the dynamic viscosity (kg m□¹ s□¹), and ν is the kinematic viscosity of the fluid (m² s□¹).

The air density required for the Reynolds number was calculated from measured air temperature and humidity. The dynamic viscosity of the air was 1.80e-5 kg m□¹ s□¹, based on the air temperature measured during the experiment. The characteristic linear dimension L is calculated by following formula:

$$\mathrm{L} = \frac{4\mathrm{A}}{\mathrm{P}} = \frac{2hw}{h+w}$$

Where, A is the slot opening area (m²), P is the perimeter of the opening (m), h is the height of the opening (m), w is the width of the opening (1.13 m).

The result of linear regression analysis of discharge coefficient with Reynolds number is given in Table 17 and Fig. 25. Regression analysis showed that the adjusted R^2 was slightly low, but the discharge coefficient decreased significantly with increasing Reynolds number (p-value = 1.07e-12).

Table 17 Regression analysis of discharge coefficient with slot opening area

Multiple R^2	Adjusted R^2	F-statistic	p-value
0.6262	0.6190	87.1	1.068e-12
	Estimate	Standard error	p-value
(intercept)	8.416e-01	3.220e-02	< 2e-16 ***
Re	-5.112e-06	5.477e-07	1.07e-12 ***

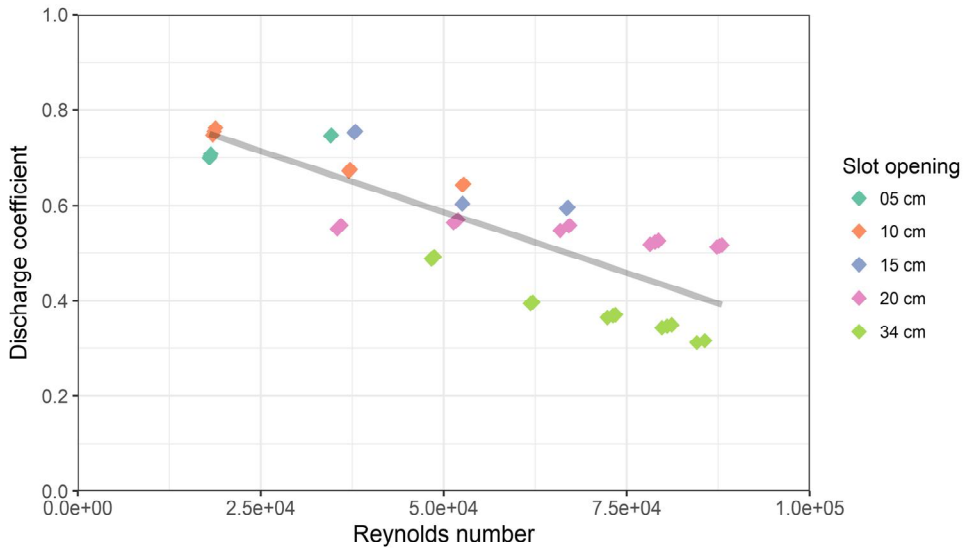

Fig. 25 Regression analysis of discharge coefficient with Reynolds number

4.3. Validation of CFD simulation model

The CFD simulation was conducted on the same condition as the field experiment in Daeseon farm. The CFD model computed ventilation rate under steady state condition. The boundary condition of slot opening was set to inlet-vent and measured discharge coefficient was applied. The manufacturer's design fan performance curve was applied to the tunnel fan boundary. Simulation results at the

same position of the field experiment (airflow of bottom center tunnel fan and static pressure difference near the control room) were compared with the measured values. Table 18 shows the relationship between the measured and CFD-simulated airflow and static pressure difference under same conditions.

Table 18 Agreement between measured and CFD simulated airflow and static pressure difference

	Airflow of central tunnel fan	Static pressure difference
Pearson correlation coefficient (R)	0.812	0.983
Root mean square error (RMSE)	1,941 CMH	2.97 Pa

A strong correlation (R = 0.812) between measured and CFD simulated airflow was observed. RMSE was calculated to be 1,941 CMH, which is 8.2% of the observed average airflow. Static pressure difference was also analyzed to have a strong correlation (R = 0.983) and small error (RMSE = 2.97 Pa). Considering the CFD simulation result, the deviation between the in-situ and design fan performance curves was dominated by the static pressure measurement position rather than the deterioration of fan due to aging.

For accurate validation of the model, multiple regression analysis was used to test the difference between measured and simulated in-situ fan performance curve. The scatter plot of measured and simulated airflow for the condition of static pressure difference over 10 Pa is shown in Fig. 26, and Table 19 shows the result of regression analysis for static pressure difference.

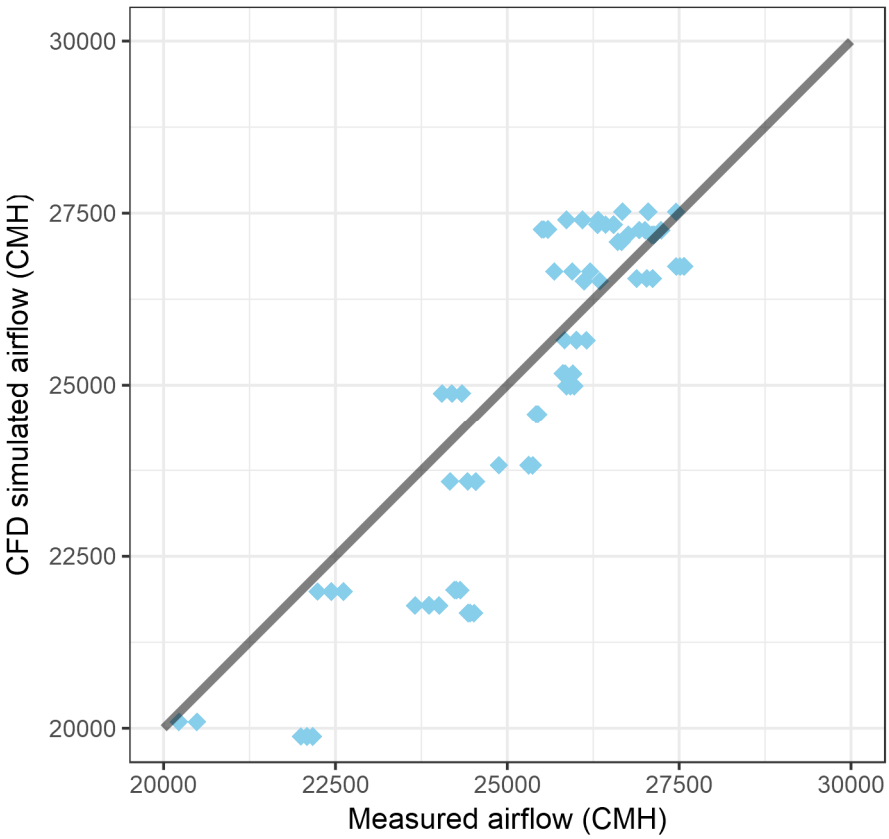

Fig. 26 Scatter plot between measured and CFD simulated airflow

Table 19 Regression analysis of static pressure difference with airflow and data acquisition method

Multiple R^2	Adjusted R^2	F-statistic	p-value
0.9092	0.9029	143.5	< 2.2e-16
	Estimate	Standard error	p-value
(intercept)	-215.7658	53.923	2.44e-04 ***
Q	90.2197	16.958	3.53e-06 ***
Q^2	-8.2209	1.3254	1.85e-07 ***
Method	5.1234	0.9144	1.38e-06 ***

Where, the dependent variable SP is the static pressure difference near control room (Pa), Q is the airflow of target tunnel fan (CMH), and *Method* is the categorical variable indicating data acquisition method (field measurement or CFD simulation).

The regression analysis was conducted with the same formula of fan performance curve, and the difference of the fan performance curve by data acquisition method tested. Regression analysis showed the difference of fan performance curve by method was statistically significant (p-value = 1.38e-06).

The in-situ fan performance curve and CFD simulation result are shown in Fig. 27. CFD simulated airflow and static pressure difference were in good agreement with the experimental result in the range where the airflow was large and the static pressure difference was low. On the contrary, the lower the airflow, the lower the agreement between measured and simulated results. The cause of the tendency can be found in the limitation of the design fan performance curve provided by the manufacturer. The design fan performance curve of the target fan (Euroemme EM50; Munters) informs only in the range of static pressure differences less than 50 Pa and airflow more than 25,000 CMH. In this study, the fan performance curve was assumed to be quadratic polynomials (Liu & Liu, 2012). If the design fan performance curve is interpreted as quadratic polynomial for out-of-data provided range, the calculated static pressure difference decreases sharply when the airflow is less than 18,700 CMH. In this study, that tendency was judged as unrealistic. The static pressure difference was assumed to be 50 Pa, which corresponds to the maximum static pressure difference provided by the manufacturer, in the range of airflow less than 25,000 CMH. However, the simulated airflow was lower than measured results under the environmental condition of airflow less than 25,000 CMH (Fig. 27). Therefore, the assumption for the static pressure difference had a limitation, and design fan performance curve should be provided in a wider range for accurate estimation of ventilation rate.

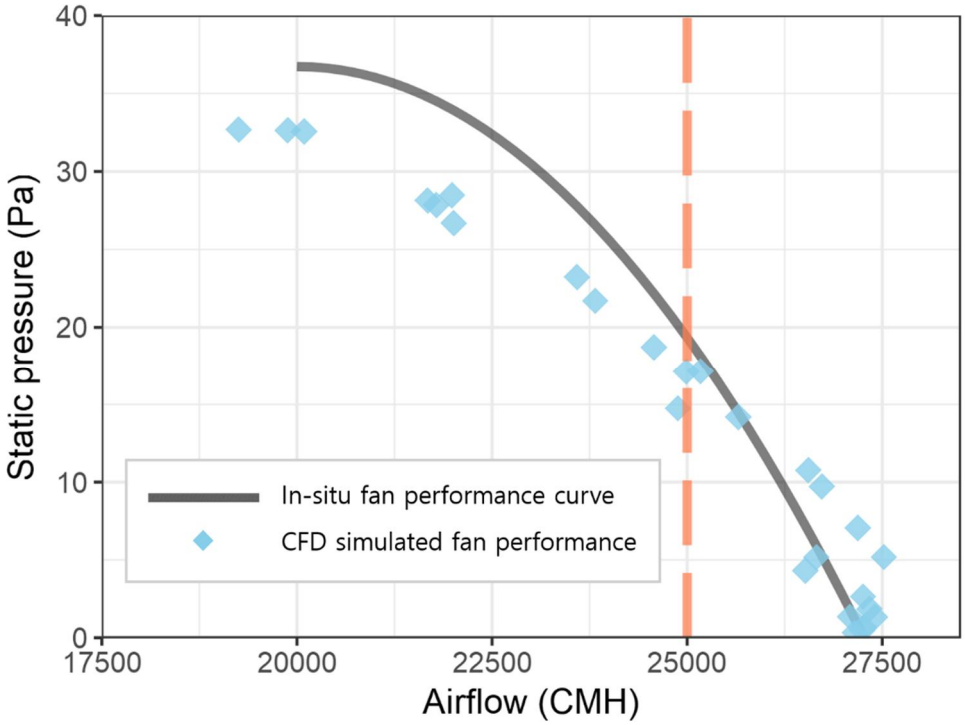

Fig. 27 Fan performance curve and CFD simulated in-situ fan performance

CFD simulation results of design fan performance curve range (airflow over 25,000 CMH) were expected to be relatively accurate. The results of validation by regression analysis within manufacturer's fan performance curve range are shown in Table 20.

Table 20 Regression analysis of static pressure difference with airflow and data acquisition method within manufacturers performance range

Multiple R^2	Adjusted R^2	F-statistic	p-value
0.9905	0.9889	625.3	< 2.2e-16
	Estimate	Standard error	p-value
(intercept)	-71.1485	32.4505	0.0417 *
Q	42.1024	10.5609	8.65e-04 ***
Q^2	-4.2478	0.8550	9.94e-05 ***
Method	0.9641	0.7912	0.2388

Where, the dependent variable ΔP is static pressure difference near control room (Pa), Q is the airflow of target tunnel fan (CMH), method is the categorical variable indicating data acquisition method (field measurement or CFD simulation).

Unlike Table 19, that regression model with the entire range of data, it was analyzed that the method variable did not significantly affect the fan performance curve (p-value = 0.2388). Therefore, the CFD model was considered to simulate the ventilation rate of the target broiler house well within the fan performance range provided by the manufacturer.

4.4. CFD simulation result

4.4.1. Static pressure distribution

The cause of the deviation between the in-situ and design fan performance curve was analyzed with CFD simulation result. As described above, the design fan performance curve was applied to the CFD model, but average static pressure difference was about 30 Pa lower than the design fan performance curve. Fig. 28 shows the example of static pressure distribution simulated by CFD.

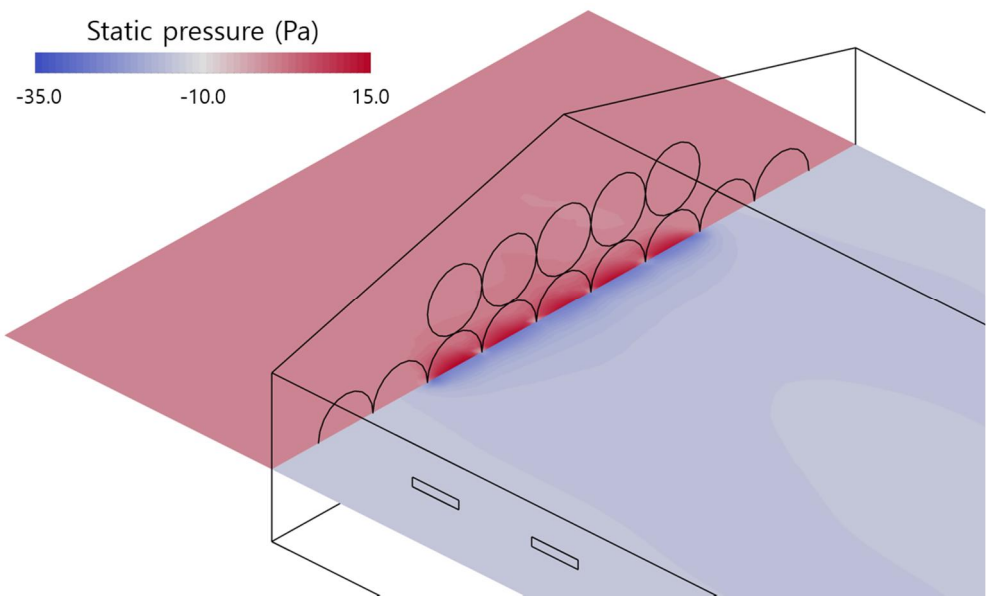

Fig. 28 Static pressure distribution near tunnel fans

Fig. 29 shows static pressure distribution on the horizontal plane of the target tunnel fan height at the same condition. The static pressure outside the broiler house was positive due to the pressure rise of the airflow passing through the exhaust fan. On the other hand, the negative static pressure was formed inside the broiler house. The static pressure difference was the largest near the tunnel fans. The maximum static pressure in the external area was 19.1 Pa, and the minimum

static pressure in the broiler house was -37.5 Pa. However, static pressure difference tended to decrease with distance from the tunnel fans.

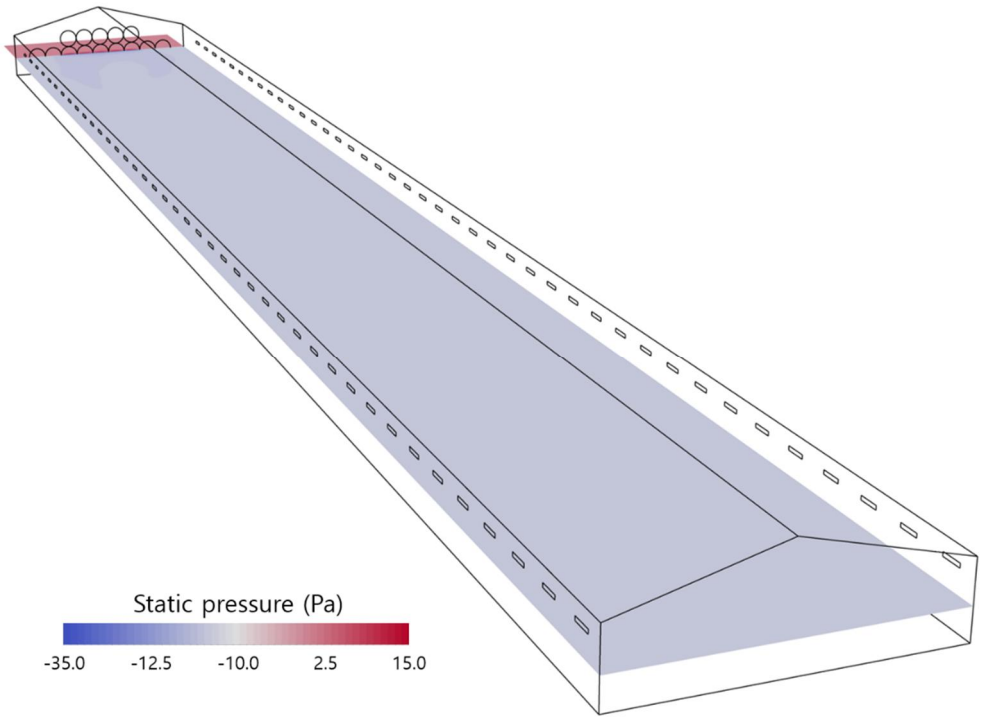

Fig. 29 Static pressure distribution of the entire broiler house

The static pressure at most locations away from the tunnel fans was constant at -14.0 Pa, and the average static pressure of the broiler house was -14.2 Pa. The static pressure outside the slot openings was set to 0 Pa. Therefore, the static pressure difference of 14.0 Pa was formed at slot openings, which is the same as that measured in the field experiment. This characteristic of static pressure distribution was the same in all CFD simulation cases. The deviation of the static pressure difference between in-situ measurement location and inlet-outlet of tunnel fan averaged 33.7 Pa (minimum 28.2 Pa to maximum 39.2 Pa) according to the airflow of tunnel fan (Fig. 19). The design fan performance curve was provided only in the range of static pressure difference less than 50 Pa. Considering the typical static pressure difference during tunnel ventilation (2.5–30 Pa; Casey et al., 2008), design fan performance curve has to be provided in a range of static pressure difference up to 70 Pa.

In general, the static pressure difference of the mechanically ventilated broiler house is measured near the control room as in the case of the target facility. The static pressure difference measured near the control room can be applied to

estimate airflow through slot openings. However, it is inappropriate for estimating airflow of exhaust fan with a design fan performance curve. It is practically difficult to measure the in-situ static pressure difference between inlet and outlet of the exhaust fan. Due to the high dynamic pressure near the exhaust fans, the static pressure is expected to be difficult to measure accurately. In addition, dust and noxious gases generated inside the broiler house may cause a failure of the static pressure sensor while discharged through the exhaust fan. Therefore, it is considered that in-situ fan performance curve (static pressure difference near the control room) should be applied instead of the design fan performance curve (fan static pressure difference) to monitor the ventilation rate.

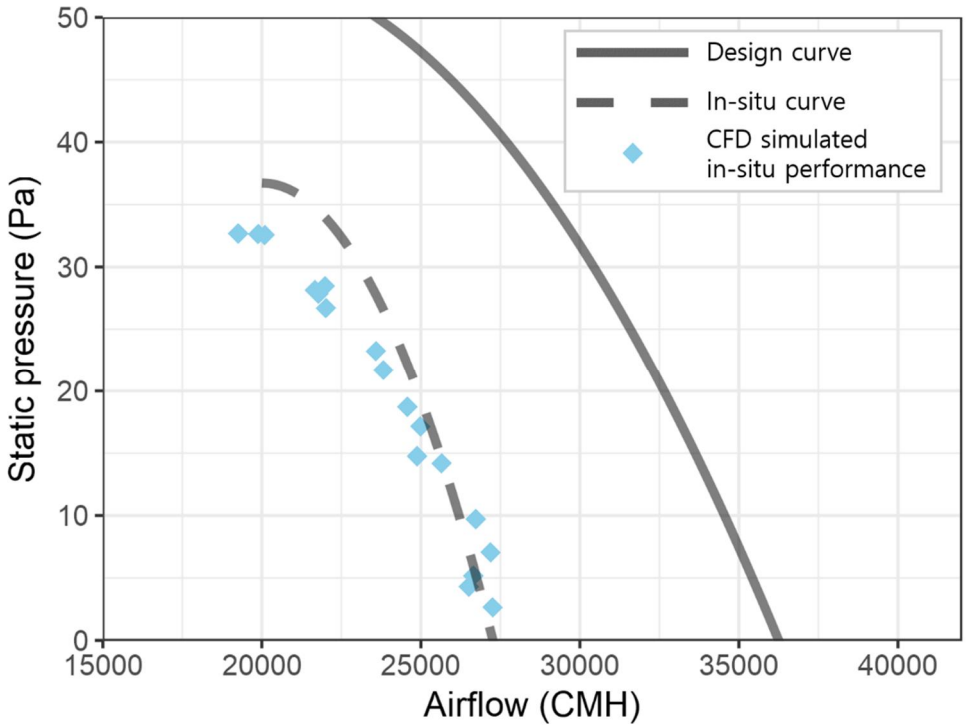

Fig. 30 Comparison of design fan performance curve (at the fan) and in-situ fan performance curve (at the in-situ measuring location)

The deviation of static pressure on the fan and average static pressure inside the broiler house is analyzed to be caused by the size difference between fan and cross-section of the broiler house. The flow through a duct of constant shape maintains the velocity of the fluid constant, and so does dynamic and static pressure. ANSI/AMCA 210 specifies that the dynamic and static pressure has to be measured in the section of the duct maintaining the constant shape. The exhaust fan installed on the wall of the livestock house corresponds to a free inlet–free outlet

type without duct. As a result, the velocity of the air decreases long the streamline due to the change of the structural shape. Therefore, there is a possibility that the distribution of the static pressure inside broiler house could be influenced by the structure of the facility.

4.4.2. In-situ fan performance curve according to length of broiler house

For analyzing the change of the in-situ fan performance curve due to the structural change, three additional models with different length were designed. The lengths of the additional models were 60, 80, and 100 m, respectively, and the slot opening area was 0.34×1.13 m (fully opened), and the remaining design method was same as the original model of target broiler house. The results of additional CFD models were compared with the original model of the same slot opening area.

Simulated data within the range of the design fan performance curve provided by the manufacturer were used for analysis. The airflow of the bottom center tunnel fan and static pressure difference near the control room are shown in Fig. 31. As with the field experiment result, the trend that airflow decreases with increasing static pressure difference was derived for all models. A multiple regression analysis was performed in the same form as the fan performance curve for testing the influence of the model length. The results are shown in Table 21.

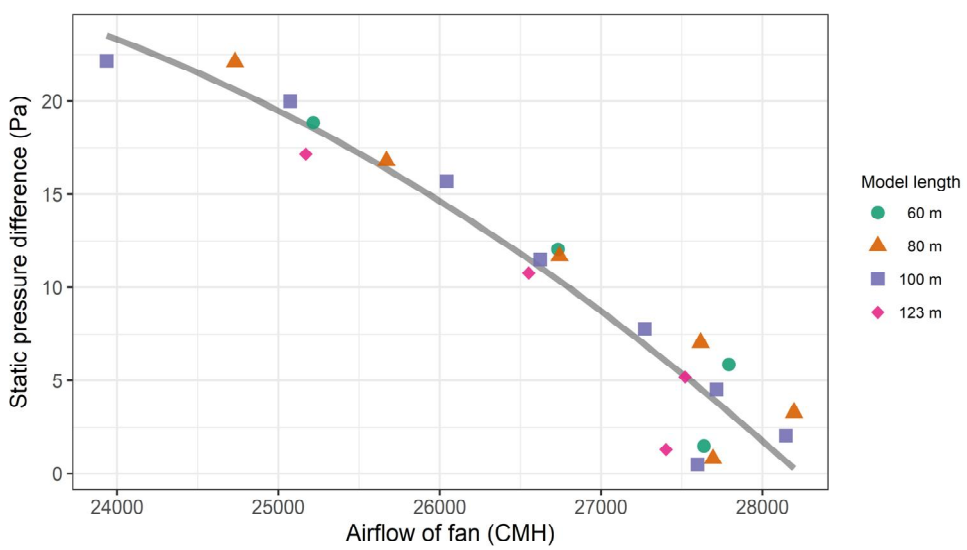

Fig. 31 Simulated in-situ fan performance curve by CFD models with different lengths of broiler houses

Table 21 Regression analysis of in-situ fan performance curve with model length

Multiple R^2	Adjusted R^2	F-statistic	p-value
0.9240	0.9133	72.94	2.879e-10
	Estimate	Standard error	p-value
(intercept)	-216.9181	244.6905	0.387
Q	84.5400	67.2237	0.225
Q^2	-7.2005	4.6065	0.135
Length	-0.0367	0.0227	0.123

Where, Q is airflow of the tunnel fan (m^3 s^{-1}), and *Length* is the length of the broiler house (m).

The linear model of the static pressure difference with second-order polynomial of the airflow and the model length was analyzed, and the p-value of the *Length* variable was 0.123. Therefore, the simulated in-situ fan performance curve was not significantly different according to the length of the CFD model (60, 80, 100, 123 m). The in-situ fan performance curve was analyzed as the inherent characteristic of the target exhaust fan—that is, not affected by the volume of the facility.

4.5. Ventilation rate formula according to the operating condition

The formula for calculating the ventilation rate according to the number of operating exhaust fans (n) and slot opening are (A) was derived from in-situ fan performance curve, orifice equation, and regression equation of discharge coefficient.

The in-situ fan performance curve is expressed as follows according to the number of operating fans.

$$\begin{aligned}\Delta P &= c_0 + c_1(Q/n) + c_2(Q/n)^2 \\ &= -241.665 + \frac{100.215}{n}\cdot Q - \frac{9.019}{n^2}\cdot Q^2\end{aligned}$$

Where, ΔP is the static pressure difference between inside and outside of the broiler house (Pa), Q is total ventilation rate (m^3 s^{-1}), and n is the number of operating fans.

The regression equation of discharge coefficient and the number of slot

openings (82) can be applied to the orifice equation as follows.

$$\mathrm{Q} = \mathrm{C_D}(82 \times A)\sqrt{\frac{2\Delta P}{\rho}}$$

$$= 82 \times (0.809 - 1.111A)A\sqrt{\frac{2\Delta P}{\rho}}$$

$$\Delta \mathrm{P} = \frac{1}{82^2(0.809 - 1.111A)^2A^2} \times \frac{\rho}{2}Q^2$$

Where, $\mathrm{C_D}$ is the discharge coefficient of slot opening (dimensionless), A is the slot opening area (m²), ρ is the air density (kg m□³)

$$\mathrm{c}_0 + \frac{c_1}{n}Q + \left(\frac{c_2}{n^2} - \frac{\rho}{2 \cdot 82^2(0.809 - 1.111A)^2A^2}\right)Q^2 = 0$$

$$\mathrm{c}_0 n^2 + c_1 n \cdot Q + \left(c_2 - \frac{\rho n^2}{2 \cdot 82^2(0.809 - 1.111A)^2A^2}\right)Q^2 = 0$$

Simplifying the coefficient of the Q² to $\mathrm{c_2}'$, the solution of the equation is calculated as follows:

$$\mathrm{c}_0 n^2 + c_1 n \cdot Q + \mathrm{c_2}' \cdot \mathrm{Q}^2 = 0$$

$$Q = \frac{-c_1 + \sqrt{c_1^2 - 4c_0 c_2'}}{2c_2'} \times n$$

The coefficient required is as follows:

$$\mathrm{c}_0 = -241.665\ \mathrm{Pa}$$

$$\mathrm{c}_1 = 100.215\ \mathrm{Pa \cdot s/m^3}$$

$$\mathrm{c}_2 = -9.019\ \mathrm{Pa \cdot s^2/m^6}$$

$$\mathrm{c}_2' = c_2 - \frac{\rho n^2}{2 \cdot 82^2(0.809 - 1.111A)^2A^2}$$

Therefore, the ventilation rate can be calculated according to the operating condition of the broiler house (n and A), if the air density ρ is assumed or calculated using air temperature and humidity. The static pressure difference of the broiler house can be derived through a similar procedure. When the air density is assumed to be 1.225 kg m□³, the ventilation rate and static pressure difference of the broiler house according to the number of operating tunnel fans (1-14) and slot

opening height (2 - 34 cm by 2 cm) were calculated as shown in Fig. 32 and Fig. 33.

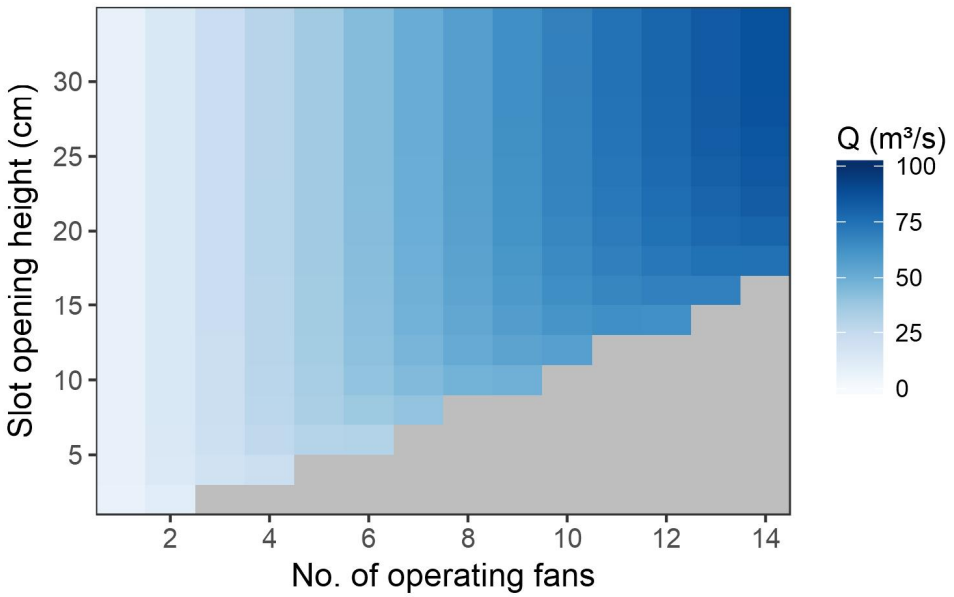

Fig. 32 Estimated ventilation rate according to operating condition of broiler house

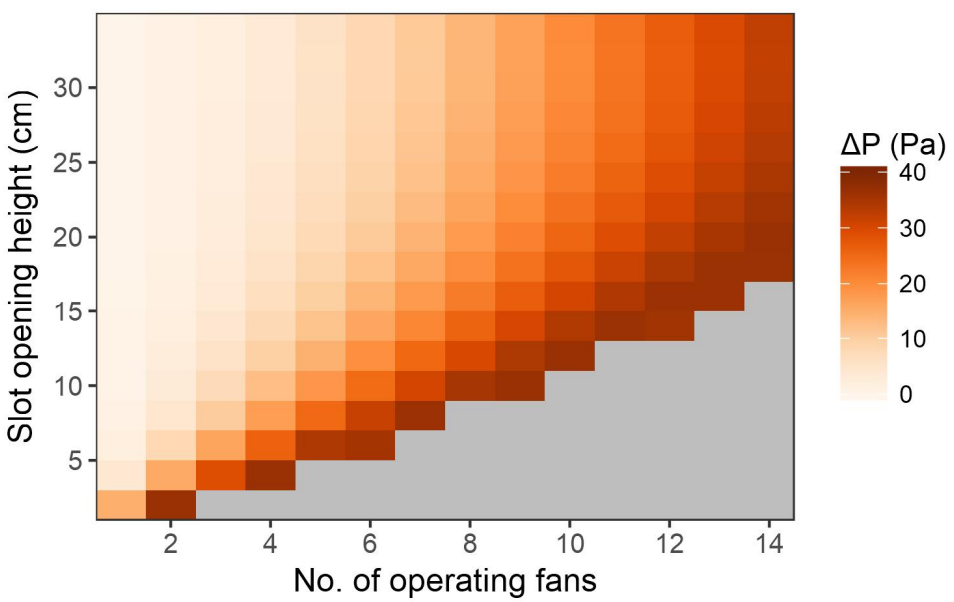

Fig. 33 Estimated average static pressure difference according to operating condition of broiler house

The gray area at the bottom right of the figure indicates the conditions that

excessive static pressure difference occur and the exhaust fans may fail. The limit slot opening height considering static pressure difference is shown in Table 22.

Table 22 Minimum limits of slot opening height according to number of operating tunnel fans

No. of operating tunnel fans	Slot opening height (cm)	No. of operating tunnel fans	Slot opening height (cm)
1	2	8	10
2	2	9	10
3	4	10	12
4	4	11	14
5	6	12	14
6	6	13	16
7	8	14	18

The ventilation rate of the target broiler house was mainly influenced by the number of operating fans, and the static pressure difference was dominated by both number of operating fans and slot opening area. The airflow of tunnel fan when slot opening height is 20 cm is 91.23–99.97% of airflow of fully opened (34 cm) condition, On the other hand, the static pressure difference when slot opening height is 20 cm is 112.8–135.4% of the static pressure difference of the fully opened condition.

In the summer season, when the slot openings are generally fully opened, it is considered that only number and cycle of operating fans should be sufficient in ventilation control. It was found that the slot opening area does not have a dominant influence on the ventilation rate when the opening height is more than 20 cm. On the other hand, jet drop distance has to be increased to prevent cold stress due to the inlet air in winter season or night (Zhang & Strøm, 1999; Kwon et al., 2015). For this purpose, the static pressure difference should be maintained above a certain level for high-velocity inlet flow. The typical static pressure difference of mechanically ventilated broiler house is 10 - 25 Pa (Casey et al., 2008). Table 23 shows the slot opening height for forming the typical range of static pressure difference in target broiler house. The static pressure difference was calculated to be at least 26.5 Pa when the all 12 tunnel fans were operated, which exceed the range.

Table 23 Slot opening height range for adequate static pressure difference according to the number of operating tunnel fans

No. of operating tunnel fans	Slot opening height (cm)	No. of operating tunnel fans	Slot opening height (cm)
1	2	8	16-34
2	2	9	18-34
3	6-8	10	22-34
4	8-10	11	26-34
5	8-14	12	-
6	10-20	13	-
7	14-34	14	-

The existing mechanically ventilated broiler houses utilize measured static pressure difference only for controlling the slot opening area. The ventilation rate was controlled only considering design maximum airflow and number of operating fans, and information on the actual amount of ventilation rate was insufficient. Although evaluation of ventilation rate considering static pressure difference is required, the measurement of the static pressure difference has a high possibility of error due to the flow around the sensor. It is expected that accurate ventilation operation will be possible by adjusting the number of operating fans and slot opening area, through the formula suggested in this study.

Chapter 5. Conclusion

In this study, a field experiment and CFD simulation were conducted to evaluate ventilation characteristics of a mechanically ventilated broiler house and derive the ventilation rate formula. Measurement of airflow of sidewall fans in a mechanically ventilated broiler house located in Buyeo showed that the airflow decreased as the number of operating sidewall fans increased. The slot opening of target broiler house was 25% open during experiment according to the winter ventilation setting. It was analyzed that the ventilation rate decreased due to the excessive static pressure difference between inside and outside of broiler house, which caused by narrow slot opening area. The measured total ventilation rate was 77.0% of the set ventilation rate. Therefore, the estimation method of ventilation rate according to the ventilation system operation and the static pressure difference is considered necessary.

The experiment was conducted for measuring the airflow of tunnel fan and the static pressure difference between inside and outside of the mechanically ventilated broiler house located in Gimje. Through the analysis of the experimental result, the in-situ fan performance curve and discharge coefficient of slot opening were evaluated. The discharge coefficient was calculated by the airflow through slot opening and static pressure difference, and it showed a large variability of 0.344–0.743. The discharge coefficient and slot opening area showed a negative correlation, and the relationship between them was analyzed by linear regression model (R^2=0.851). The in-situ fan performance curve was calculated by regression model with airflow through exhaust fan and static pressure difference (R^2=0.900). The static pressure difference of the in-situ fan performance curve was on average 33.7 Pa lower than the design fan performance curve provided by the manufacturer. The deviation between the two curves was analyzed as resulting from the measurement position of the static pressure.

The CFD model of the target broiler house was designed to overcome the limitation of the field experiment. The simulation was conducted for the same conditions with the field experiment. The CFD model validation was conducted by comparing the airflow of target exhaust fan according to the ventilation operating condition. Statistical analysis showed no significant difference between the measured and simulated airflow (p-value = 0.239). Therefore, it was possible to simulate the change of ventilation rate of the mechanically ventilated broiler house according to the ventilation operating condition. Additional CFD simulations with broiler house models of different lengths were conducted. A statistically significant difference of in-situ fan performance curve according to the length of broiler house was not observed by CFD simulation (p-value = 0.189). Therefore, the in-situ fan

performance curve measured in this study is considered applicable regardless of the length and volume of the broiler house.

The ventilation rate formula was derived from the in-situ fan performance curve, orifice equation, and regression equation of the discharge coefficient. The ventilation rate and static pressure difference can be estimated by the formula according to the number of operating exhaust fans and slot opening area. It is expected that ventilation rate can be estimated by the operating condition of the facility, which is relatively easy to measure compared to the direct measurement of airflow. In this study, ventilation characteristics were evaluated for a single mechanically ventilated broiler house. The methodology of this study can be applied to evaluate the ventilation characteristics of other mechanically ventilated broiler or pig houses. It is expected that the correlation between the in-situ and design fan performance curve can be analyzed through CFD simulation using various exhaust fans.

Bibliography

Albright, L. (1976). Air flow through hinged baffle slotted inlets. *Transactions of the ASAE, 19*(4), 728-0732.

American Society of Heating, R., & Engineers, A.-C. (2001). *2001 ASHRAE Handbook: Fundamentals*: ASHRAE.

Andersen, K. T. (2002). Friction and contraction by ventilation openings with movable flaps. *Proceedings of Roomvent 2002, Copenhagen, Denmark*.

Bombik, T., Biesiada-Drzazga, B., Bombik, E., & Frankowska, A. (2011). The influence of temperature and humidity conditions on productivity and welfare of broiler chickens. *Acta Scientiarum Polonorum. Zootechnica, 10*(4).

Bottcher, R., Singletary, I., & Baughman, G. (1992). Ventilation of Poultry Buildings with Exhaust Fans at One End and Continuous Slot Inlets along The Sidewalls. *Transactions of the ASAE, 35*(5), 1673-1679.

Calvet, S., Cambra-López, M., Blanes-Vidal, V., Estellés, F., & Torres, A. (2010). Ventilation rates in mechanically-ventilated commercial poultry buildings in Southern Europe: Measurement system development and uncertainty analysis. *Biosystems Engineering, 106*(4), 423-432.

Calvet, S., Gates, R. S., Zhang, G., Estellés, F., Ogink, N. W., Pedersen, S., & Berckmans, D. (2013). Measuring gas emissions from livestock buildings: a review on uncertainty analysis and error sources. *Biosystems Engineering, 116*(3), 221-231.

Casey, K., Ford, S., McClure, J., Zhang, Y., & Gates, R. (2007). Determining fan performance using FANS: an investigation of performance impacts. *Applied engineering in agriculture, 23*(3), 333-338.

Casey, K., Gates, R., Wheeler, E., Xin, H., Liang, Y., Pescatore, A., & Ford, M. (2008). On-farm ventilation fan performance evaluations and implications. *Journal of applied poultry research, 17*(2), 283-295.

Fluent. (2009). Fluent 12.0 User's guide. *Ansys Inc*.

Ford, S., & Riskowski, G. (2003). Effect of windbreak wall location on ventilation fan performance. *Applied engineering in agriculture, 19*(3), 343.

Gates, R. S., Casey, K. D., Xin, H., Wheeler, E. F., & Simmons, J. D. (2004). Fan assessment numeration system (FANS) design and calibration specifications. *Transactions of the ASAE, 47*(5), 1709.

Gates, R., Xin, H., Casey, K., Liang, Y., & Wheeler, E. (2005). Method for measuring ammonia emissions from poultry houses. *Journal of applied poultry research, 14*(3), 622-634.

Harvey, T., & Belle, B. (2016). A Field Evaluation of a Main Axial Ventilation Fan to Establish Stall Zone and Fan Performance Curve.

Hatem, M. H., Abdelbary, K. M., Mohamed, B. A., & haddy Ahmed, N. A. (2011). *The Productive And Reproductive Performance Of Rabbits In Different Housing Systems*. Paper presented at the 2011 Louisville, Kentucky, August 7-10, 2011.

Heiselberg, P., & Sandberg, M. (2006). Evaluation of discharge coefficients for window openings in wind driven natural ventilation. *International Journal of Ventilation, 5*(1), 43-52.

Karava, P., Stathopoulos, T., & Athienitis, A. (2004). Wind driven flow through openings–a review of discharge coefficients. *International Journal of Ventilation, 3*(3), 255-266.

Kiwan, A., Berg, W., Fiedler, M., Ammon, C., Gläser, M., Müller, H.-J., & Brunsch, R. (2013). Air exchange rate measurements in naturally ventilated dairy buildings using the tracer gas decay method with 85 Kr, compared to CO 2 mass balance and discharge coefficient methods. *Biosystems Engineering, 116*(3), 286-296.

Knížatová, M., Mihina, Š., Brouček, J., Karandušovská, I., & Mačuhová, J. (2010). The influence of litter age, litter temperature and ventilation rate on ammonia emissions from a broiler rearing facility. *Czech Journal of Animal Science, 55*(8), 337-345.

Korea Rural Economic Institute. (2017). *Agricultural Outlook 2017*: Korea Rural Economic Institute.

Kwon, K.-S., Lee, I.-B., & Ha, T. (2016). Identification of key factors for dust generation in a nursery pig house and evaluation of dust reduction efficiency using a CFD technique. *Biosystems Engineering, 151*, 28-52.

Kwon, K.-S., Lee, I.-B., Zhang, G. Q., & Ha, T. (2015). Computational fluid dynamics analysis of the thermal distribution of animal occupied zones using the jet-drop-distance concept in a mechanically ventilated broiler house. *Biosystems Engineering, 136*, 51-68.

Kwon, K. S., Jo, Y. S., Lee, I. B., Ha, T. H., & Hong, S. W. (2014). Measurement of Dust Concentration in a Mechanically Ventilated Broiler House and Analysis of Dust Generation from Ground Beds. *Journal of the Korean Society of Agricultural Engineers, 56*(6), 31-43.

Lakenman, K., Segura, J., Atkins, R., Ben-Zvi, M., & Feddes, J. (2004). *Measuring ventilation rates in livestock buildings with an averaging Pitot tube.* Paper presented at the 2004 ASAE Annual Meeting.

Lara, L. J., & Rostagno, M. H. (2013). Impact of heat stress on poultry production. *Animals, 3*(2), 356-369.

Li, H., Rong, L., Zong, C., & Zhang, G. (2016). A numerical study on forced convective heat transfer of a chicken (model) in horizontal airflow. *Biosystems Engineering, 150*, 151-159.

Li, H., Xin, H., Liang, Y., Gates, R. S., Wheeler, E. F., & Heber, A. J. (2005). Comparison of direct vs. indirect ventilation rate determinations in layer barns using manure belts. *Transactions of the ASAE, 48*(1), 367-372.

Liang, Y., Bautista, R., & Costello, T. A. (2016). Validating a multi-port, averaging pitot tube for measuring fan airflow rates. *Applied engineering in agriculture, 32*(4), 409-415.

Liang, Y., Bautista, R., Dabhadkar, G., & Costello, T. A. (2013). *Validating an Averaging Pitot Tube for Measuring Fan Air Flow Rates*. Paper presented at the 2013 Kansas City, Missouri, July 21-July 24, 2013.

Lin, X.-J., Cortus, E., Zhang, R., Jiang, S., & Heber, A. (2011). Ventilation monitoring of broiler houses in California. *Transactions of the ASABE, 54*(3), 1059-1068.

Liu, G., & Liu, M. (2012). Development of simplified in-situ fan curve measurement method using the manufacturers fan curve. *Building and Environment, 48*, 77-83.

Liu, G., Joo, I.-S., Song, L., & Liu, M. (2003). Development of In-situ Fan Curve Measurement with One Airflow Measurement.

Liu, M., Liu, G., Joo, I., Song, L., & Wang, G. (2005). Development of in situ fan curve measurement for VAV AHU systems. *Transactions of the ASME-N-Journal of Solar Energy Engineering, 127*(2), 287-293.

Ministry of Agriculture, Food and Rural Affairs. (2016). *Agriculture, Food and Rural Affairs Statistical Yearbook*. Sejong: Ministry of Agriculture, Food and Rural Affairs.

Morello, G. M., Overhults, D. G., Gates, R. S., Day, G. B., Lopes, I. M., & Earnest, J. W. (2014). Using the Fan Assessment Numeration System (FANS) in Situ: A Procedure for Minimizing Errors During Fan Tests. *Transactions of the ASABE, 57*(1), 199-209.

Mostafa, E., Lee, I.-B., Song, S.-H., Kwon, K.-S., Seo, I.-H., Hong, S.-W., . . . Han, H.-T. (2012). Computational fluid dynamics simulation of air temperature distribution inside broiler building fitted with duct ventilation system. *Biosystems Engineering, 112*(4), 293-303.

Pawar, S., Cimbala, J., Wheeler, E., & Lindberg, D. (2007). Analysis of poultry house ventilation using computational fluid dynamics. *Transactions of the ASABE, 50*(4), 1373-1382.

Pearson, C., & Owen, J. (1994). The resistance to air flow of farm building ventilation components. *Journal of Agricultural Engineering Research, 57*(1), 53-65.

Pedersen, S., Takai, H., Johnsen, J. O., Metz, J., Koerkamp, P. G., Uenk, G., . . . Short, J. (1998). A comparison of three balance methods for calculating ventilation rates in livestock buildings. *Journal of Agricultural Engineering Research, 70*(1), 25-37.

Rojano, F., Bournet, P.-E., Hassouna, M., Robin, P., Kacira, M., & Choi, C. Y. (2015). Modelling heat and mass transfer of a broiler house using computational fluid dynamics. *Biosystems Engineering, 136*, 25-38.

Roumeliotis, T. S., Dixon, B. J., & Van Heyst, B. J. (2010). Characterization of gaseous pollutant and particulate matter emission rates from a commercial broiler operation part I: Observed trends in emissions. *Atmospheric Environment, 44*(31), 3770-3777.

Segura, J., Feddes, J., Ouellette, C., & Ben-Zvi, M. (2005). *Development of a Multi-port Averaging Pitot Tube System for Measuring Ventilation Rates Under Field Conditions*. Paper presented at the 2003, 2004, 2005 Pacific Northwest Region Papers.

Seo, I.-H., Lee, I.-B., Chang, P.-W., Hwang, H.-S., Hong, S.-W., & Lee, S.-Y. (2006). *Study on ventilation system of naturally ventilated broiler house by aerodynamic approach.* Paper presented at the 2006 ASAE Annual Meeting.

Seo, I.-H., Lee, I.-B., Moon, O.-K., Kim, H.-T., Hwang, H.-S., Hong, S.-W., . . . Kim, Y.-H. (2009). Improvement of the ventilation system of a naturally ventilated broiler house in the cold season using computational simulations. *Biosystems Engineering, 104*(1), 106-117.

Shen, X., Zhang, G., & Bjerg, B. (2012). Comparison of different methods for estimating ventilation rates through wind driven ventilated buildings. *Energy and Buildings, 54*, 297-306.

Statistics Korea. (2017). Livestock survey. Retrieved from http://kosis.kr

Timmons, M., Irish, W., & Toleman, W. (1986). Temperature Variations Within Caged-Layer Housing as Affected by Inlet Flow Characteristics. *Applied engineering in agriculture, 2*(2), 153-157.

Winkel, A., Mosquera, J., Koerkamp, P. W. G., Ogink, N. W., & Aarnink, A. J. (2015). Emissions of particulate matter from animal houses in the Netherlands. *Atmospheric Environment, 111*, 202-212.

Wood, D., Cowherd, S., & Van Heyst, B. (2015). A summary of ammonia emission factors and quality criteria for commercial poultry production in North America. *Atmospheric Environment, 115*, 236-245.

Wu, Z. (2009). *Modeling, Estimation and Control of Indoor Climate in Livestock Buildings*. Videnbasen for Aalborg UniversitetVBN, Aalborg UniversitetAalborg University, Det Teknisk-Naturvidenskabelige FakultetThe Faculty of Engineering and Science, Institut for Elektroniske SystemerDepartment of Electronic Systems.

Xin, H., Li, H., Burns, R., Gates, R., Overhults, D., & Earnest, J. (2009). Use of CO2 concentration difference or CO2 balance to assess ventilation rate of broiler houses. *Transactions of the ASABE, 52*(4), 1353-1361.

Zhang, G.-Q., Pedersen, S., & Kai, P. (2010). *Uncertainty analysis of using CO 2 production models by cows to determine ventilation rate in naturally ventilated buildings*. Paper presented at the World Congress of the International Commission of Agricultural Engineering (CIGR), Sustainable biosystems through engineering.

Zhang, G., & Strøm, J. S. (1999). Jet drop models for control of non-isothermal free jets in a side-wall multi-inlet ventilation system. *Transactions of the ASAE, 42*(4), 1121.

국문 초록

국내 농업 생산액 중 축산업이 차지하는 비율은 1990년대 이래 꾸준히 증가하고 있다. 그 중에서도 닭고기의 생산량은 지속적으로 증가하는 1인당 소비량에 따라 상승하는 경향을 보이고 있다. 증가하는 닭고기 소비량을 충족시키기 위해 육계 사육 형태는 생산량 증대를 위한 대형화와 밀집화를 추구하고 있다. 그러나 육계의 밀집 사육 시 축산 시설 내부의 열과 수분, 그리고 오염물질의 축적을 초래하며, 부적절한 사육 환경의 조성은 생산성의 하락으로 이어진다. 시설 내부 환경 조절의 실패 시, 고온 및 저습 환경으로 인한 탈수 증상, 고습한 환경으로 인한 병원성 미생물의 증식, 오염물질의 축적으로 인한 육계의 면역력 하강 등의 문제점이 발생할 수 있다.

고도의 시설 환경 조절을 통한 생산 효율 향상을 위하여 강제환기식 사육 시설과 자동 제어 시스템이 도입되고 있는 추세이다. 강제환기식 육계사는 축산 시설의 주요 환경 조절 메커니즘인 환기의 제어 측면에서 이점을 지닌다. 환기는 시설 내부에서 발생한 열과 수분, 오염물질을 배출시키는 역할을 수행한다. 적절한 양의 대상 물질을 배기 시키기 위해선 시설 내외 환경 조건과 더불어 환기량의 정확한 평가가 요구된다. 현재 강제환기식 육계사의 설정 환기량은 배기팬의 최대 유량 및 가동 대수와 시간을 통해 산정되고 있다. 그러나 실제 배기팬의 유량은 입기구의 면적 감소와 그에 따른 시설 내외 정압력 차이의 증가에 따라 저감된다. 이를 고려하여 배기팬의 환기 특성인 팬 성능 곡선과 입기구의 특성인 오리피스 공식을 고려한 강제환기식 시설의 환기량의 산정 방식이 제안된 바 있다. 그러나 육계사를 대상으로 한 팬 성능 곡선 및 오리피스 공식의 계수인 유출 계수의 평가 연구는 부족한 실정이다.

이에 본 연구에서는 두 강제환기식 육계사를 대상으로 환기 시설의 운영 조건에 따른 환기량의 변화를 평가하였다. 동절기 육계사의 설정 환기량 대비 환기량 감소를 평가하기 위하여 부여군에 위치한 강제환기식 육계사의 측벽 배기팬 유량을 측정하였다. 그 결과 배기팬의 가동 대수가 증가할수록 하나의 배기팬을 통과하는 유량이 감소하는 것으로 나타났다. 3대의 측벽 배기팬을 모두 가동하였을 경우 유량은 설정 환기량 대비 77.0% 수준으로 평가되었다. 실험 당시 대상 시설은 동절기 시설 운영 조건에 따라 입기 슬롯을 25% 개방하고 있었다. 좁은

입기 면적으로 인해 형성된 시설 내외 정압력 차이가 배기팬에 부하로 작용하여 환기량이 감소한 것으로 분석된다.

강제환기식 육계사의 환기 특성 분석 및 환기량 산정 방안의 도출을 위하여 김제시에 위치한 강제환기식 육계사를 대상으로 실험을 수행하였다. 대상 시설의 터널팬 가동 대수 및 입기 슬롯의 개방 면적에 따른 터널팬의 유량 및 시설 내외 정압력 차이를 측정하였다. 현장 실험의 한계를 보완하기 위해 대상 시설의 전산유체역학 모델을 설계하였으며, 현장 실험과 동일한 환기 시설 운영 조건에 대한 시뮬레이션을 수행하였다. 모델 검증을 위해 배기팬 유량을 대상으로 회귀분석을 시행한 결과, 실측치와 모의치 간 유의한 차이가 관측되지 않았다 (p-value = 0.239).

측정된 환기량과 정압차를 분석하여 배기팬의 환기 특성인 현장 팬 성능 곡선과 입기 슬롯의 환기 특성인 유출 계수를 산정하였다. 분석 결과 현장 팬 성능 곡선은 제조사에서 제공하는 설계 팬 성능 곡선에 비해 평균 33.7 Pa 낮은 정압차가 나타났다. 전산유체역학 시뮬레이션 결과 시설 내부 정압력의 분포 특성으로 인하여 현장 및 설계 팬 성능 곡선의 차이가 발생하는 것으로 분석되었다. 배기팬의 흡입구와 배출구 간 정압차는 설계 팬 성능 곡선에 따라 상대적으로 높은 수치가 형성되었다. 반면 현장 실험의 정압 측정 위치를 포함한 나머지 대부분의 공간에서 배기팬 인근에 비해 감소된 정압차가 일정하게 유지되었다. 대상 시설과 다른 길이의 강제환기식 육계사 모델을 추가적으로 설계하여 분석한 결과, 시설 길이에 따 현장 팬 성능 곡선의 유의한 차이가 나타나지 않았다 (p-value = 0.189). 따라서 현장 측정한 팬 성능 곡선은 대상 배기팬의 고유한 특성인 것으로 분석된다. 입기 슬롯의 유출 계수 산정 결과, 개방 면적의 감소에 따라 유출 계수는 최소 0.344에서 최대 0.743까지 증가하였으며, 이는 일반적으로 사용되는 환기창의 유출 계수 추정치 (0.65)의 5.29%-114.3% 수준이다. 유출 계수의 일반적인 적용을 위해 회귀 분석을 통하여 입기 슬롯의 유출 계수와 개방 면적 간 선형 관계식을 도출하였다 (R^2=0.851). 현장 실험을 통해 측정한 현장 팬 성능 곡선, 오리피스 공식, 유출 계수의 회귀식을 통하여 환기량 및 정압력의 산정 공식을 유도하였다. 고가의 장비를 통한 환기량 및 저압력의 직업 측정 대신 본 연구에서 제시한 산정 공식을 통하여 배기팬의 가동 대수 및 입기 면적에 따른 환기량을 평가할 수 있을 것으로 기대된다.

Keyword: Computational fluid dynamics, Discharge coefficient, Fan performance curve, Mechanical ventilation, Broiler house, Orifice equation

Student Number: 2016-21704